Activation of the proton sensing G-protein coupled receptor, GPR4, regulates focal adhesion dynamics and delays cell spreading due to increased cytoskeletal tension

by

Calvin Richard Justus

June, 2013

Director of Thesis: Li Yang

Major Department: Oncology

The tumor microenvironment is characteristically acidic due to insufficient blood perfusion, chronic inflammation, hypoxia, and altered cell metabolism. The low pH found in the tumor microenvironment may facilitate the dissemination of cancer cells into the blood stream or lymph system by breaking down extracellular matrix components and degrading the basement membrane. In the murine B16F10 melanoma model, low pH has also been reported to activate the proton sensing G-protein coupled receptor, GPR4, and decrease cell migration in vitro as well as reduce pulmonary metastasis subsequent to tail vein injections. In this study we investigated delayed cell spreading found in B16F10 melanoma cells genetically modified to express GPR4 at a high level, namely B16/GPR4 cells. Attachment assays to tissue culture plates, fibronectin, glass coverslips, and matrigel established that B16/GPR4 cell spreading was significantly delayed when plated in media buffered to pH 6.4. Next, we investigated the specific heterotrimeric G-protein responsible for delayed B16/GPR4 cell spreading by using several chemical activators and inhibitors as well as numerous genetically engineered cell lines. Treatment with either C3-transferase (CT04), a direct Rho inhibitor, or a $G_{12/13}$ inhibitory construct restored B16/GPR4 cell spreading significantly to a level similar to the vector control group and the physiological pH treatment group. We also evaluated the G_s and G_q G-protein

pathways by using 2', 5'-dideoxyadenosine (DDA) and 8-bromo-cAMP or thapsigargin and a G_q inhibitory construct but found little modifications in B16/GPR4 cell spreading indicating the $G_{12/13}$ G-protein pathway as the responsible variant. The downstream signaling mechanisms for delayed B16/GPR4 cell spreading were investigated. Both the ROCK inhibitor, Y27632, and the MLCK inhibitor staurosporine restored cell spreading. The same chemical inhibitors and activators as well as inhibitory constructs that restored B16/GPR4 cell spreading also reduced the formation of actin stress fibers indicating a proton-induced signaling cascade, which leads to increased cytoskeletal tension and delayed cell spreading. Due to the importance of focal adhesion dynamics in cell spreading and migration we next investigated two focal adhesion proteins that are vital for this process, phospho-paxillin (Y118) and phospho-focal adhesion kinase (Y397). The spatial localization of phospho-paxillin (Y118) and phospho-FAK (Y397) in B16/GPR4 cells after one-hour attachment assays is altered when treated with acidic media, displaying localization to the cell body instead of the cell periphery where dynamic focal adhesions are located. These results indicate that a proton-induced GPR4/$G_{12/13}$/Rho/Rock/MLCK signaling pathway is responsible for delayed melanoma cell spreading and altered focal adhesion dynamics.

Activation of the proton sensing G-protein coupled receptor, GPR4, regulates focal adhesion dynamics and delays cell spreading due to increased cytoskeletal tension

A Thesis

Presented To the Faculty of the Department of Oncology

East Carolina University

In Partial Fulfillment of the Requirements for the Degree

Interdisciplinary Biomedical Science

by

Calvin Richard Justus

June, 2013

Activation of the proton sensing G-protein coupled receptor, GPR4, regulates focal adhesion dynamics and delays cell spreading due to increased cytoskeletal tension.

by

Calvin Richard Justus

APPROVED BY:

DIRECTOR OF
DISSERTATION/THESIS: _____
Li Yang, Ph.D.

COMMITTEE MEMBER: _____
Kathryn Verbanac, Ph.D.

COMMITTEE MEMBER: _____
Maria Ruiz-Echevarria, Ph.D.

COMMITTEE MEMBER: _____
Qun Lu, Ph.D.

PROGRAM DIRECTOR:_____
Richard Franklin, Ph.D.

DEAN OF THE
GRADUATE SCHOOL: _____
Paul J. Gemperline, Ph.D.

Acknowledgements

It is a pleasure to thank all of those who made this thesis possible. I owe my deepest gratitude to Dr. Yang, a great scientist whose work ethic is bypassed by no one. Thank you for directing me in my studies and providing me with the opportunity to work under your supervision. Furthermore, I would like to thank my thesis committee for their input and advice throughout the duration of my project. I would also like to thank Nancy and Ivy for all their time and patience during my training. To my parents Debora and George, I want to thank you for always believing in me. To my new wife Jessica Justus, it's been a wild ride and thank you for all of your support. Finally, I offer my regards and blessings to all my friends, family, and colleagues who supported me in the completion of my degree.

Calvin Justus

TABLE OF CONTENTS

LIST OF FIGURES

LIST OF TABLES AND DIAGRAMS

LIST OF SYMBOLS OR ABBREVIATIONS

8b	-8-bromo cAMP
AC	-Adenylyl Cyclase
Ca^{2+}	-Calcium
cAMP	-Cyclic Adenosine Monophosphate
cDNA	-Complimentary Deoxyribonucleic Acid
CN01	-Calpeptin
CT04	-C3-Transferase
DAPI	-4', 6-diamidino-2-phenylindole
DDA	-2', 5'-dideoxyadenosine
DMEM	-Dulbecco's Modified Eagle Medium
DPBS	-Dulbecco's Phosphate Buffered Saline
EGFP	-Enhanced Green Fluorescent Protein
FAK	-Focal Adhesion Kinase
FBS	-Fetal Bovine Serum
FOV	-Field of View
Gα	-Alpha Subunit of G-protein
Gβ	-Beta Subunit of G-protein
Gγ	-Gamma Subunit of G-protein
GAP	-GTPase Activating Protein
GDP	-Guanosine Diphosphate
GEF	-Guanine Nucleotide Exchange Factor
GPCR	-G-protein Coupled Receptor
GRK	-G-protein Related Kinase

GTP -Guanosine Triphosphate

H^+ -Hydrogen

ICC -Immunocytochemistry

LUT -Look Up Table

mAb -Monoclonal Antibody

MLC -Myosin Light Chain

MLCK -Myosin Light Chain Kinase

Na^+ -Sodium

Ⓟ -Phosphate Group

P115 -P115-Rho Guanine Nucleotide Exchange Factor

PEG -Polyethylene Glycol

PKA -Protein Kinase A

PKC -Protein Kinase C

RGS -Regulator of G-protein Signaling

ROCK -Rho-Kinase

STA -Staurosporine

TG -Thapsigargin

TRAIL -TNF-Related Apoptosis Inducing Ligand

Y27 -Y27632

Y118 -Tyrosine 118

Y397 -Tyrosine 397

Chapter 1: Introduction

The Hallmarks of Cancer

Cancer may be defined as a collection of diseases that is portrayed by uninhibited cell division and spread of malignant cells (2). To demonstrate the heavy presence of cancer in the United States, the expected new cases of cancer in 2012 was 1, 638,910 and the total estimated deaths were 577,190 (2). However, as a result of advanced biomedical research and new treatment options the five-year survival percentage has increased from 49% in the 1970's to 67% in between 2001 and 2007 (2). Even as the survival percentage of cancer patients has increased since the 1970's effective treatment options for many types of cancers are still extremely rare. To further investigate what alternative treatment options may still exist, knowledge of the hallmarks of cancer may be of tremendous importance.

In 2000, several of the known characteristics of cancer were defined in a review article entitled, The Hallmarks of Cancer (32). This review article speculated that cancer acquires six biological characteristics that contribute to the development of human tumors. The six characteristics that were described were self-sufficiency in growth signals, insensitivity to anti-growth signals, limitless replicative potential, sustained angiogenesis, tissue invasion and metastasis, and lastly evading apoptosis (32). In addition, the same group released an updated version of the hallmarks of cancer in 2011 that stressed two further biological capabilities that contribute to the multistep development of cancer such as the deregulation of cellular energetics and avoiding immune destruction (31). In this report altered cellular energetics, or in other words altered cell metabolism, is particularly important.

It has been demonstrated that in the presence of oxygen tumor cells may radically shift away from oxidative phosphorylation to glycolysis, which is a process acknowledged as the Warburg Effect (87, 88, and 89) (Diagram 1). In addition, as a result of poor blood perfusion and inadequate tumor vasculature, an absence of oxygen may promote a further metabolic shift in energy production away from oxidative phosphorylation (83, 84, and 85) (Diagram 1). As a result of increased glycolysis in tumor cells lactate is produced. To compensate for an increased intracellular concentration of lactate tumor cells will export it and accumulated protons into the extracellular space using membrane Na^+/H^+ exchangers, monocarboxylate transporters, or carbonic anhydrases (10, 22, 29, 52, 75, and 90). Proton export from the inside of the cell into the extracellular space will increase cell survival and permit cell proliferation (40, 51, and 90). In addition, proton export gradually reduces the pH of the tumor microenvironment, which causes extracellular acidosis (Diagram 1). This is opposite of that found in normal tissue where intracellular pH is more acidic than its external environment (28, 83, 84, and 85). The gradual lowering of extracellular pH in the tumor microenvironment over time may have many effects on tumor development and metastatic progression. Furthermore, how tumor cells use specific receptors to sense low extracellular pH and acidosis is a relatively new area of study in cancer research. In this study we have investigated GPR4, a receptor that senses low extracellular pH due to its ability to bind protons.

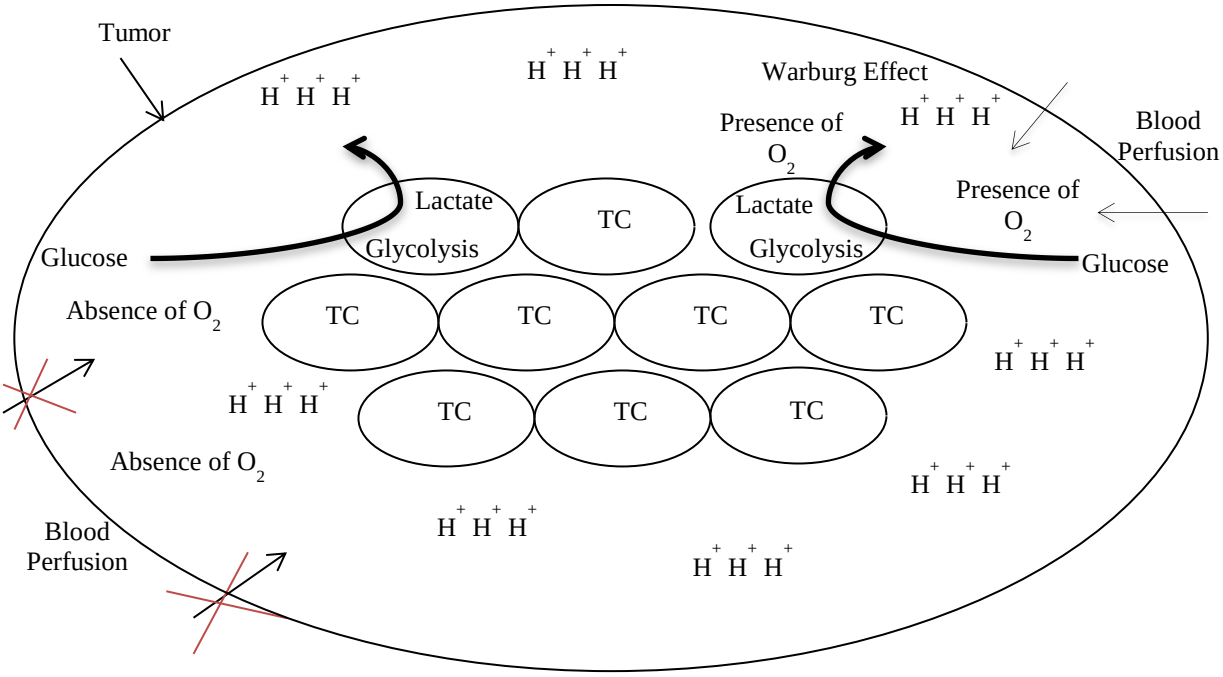

Diagram 1. The Tumor Microenvironment and Acidosis. TC-Tumor Cell.

Malignant Transformation

As a result of telomere attrition and controlled regulation of growth signals, eukaryotic cells normally have a limited lifespan. To avoid unwanted mutations and end-to-end chromosomal fusions somatic cells typically enter senescence or facilitate apoptosis after a regulated number of cell divisions (9 and 96). However, somatic cells may circumvent normal cell death and continue dividing. This may be caused by an initial stimulus such as chronic inflammation, chemical exposure, or viral infection. Aberrant stimuli may eventually generate a dynamic alteration in gene expression. A modification in gene expression may lead to the repression of tumor suppressor genes, e.g. Tumor Protein 53, or possibly amplify the expression of growth signals, e.g. Epidermal Growth Factor. Modifications in gene expression promote the opportunity for atypical cell survival and may also facilitate malignant transformation. After

achieving the ability to bypass normal cell death, malignant cells may begin to divide faster than the surrounding tissue and will eventually form a solid alien mass typically identified as a tumor.

The primary tumor, or the anatomical site where malignant transformation first occurred, begins with one cell that may have undergone one or several severe mutations. The first mutation that caused malignant transformation may ultimately cause further genetic anomalies and chromosomal instability. As the cell divides and accrues more errors in gene expression, the tumor cell population may evolve into a heterogeneous cell mass. This cell population will then evolve and the most apt for survival will be naturally selected for in a Darwinian fashion (48). The term that is used to describe this phenomenon is clonal evolution (27 and 48). An additional hypothesis is that cancer stem cells give rise to heterogeneity as a result of differentiation instead of error accumulation (21). Regardless of the mechanism, a diverse cell population may further the advancement of the tumor and may possibly lead to invasion and metastasis. The progression of clonal evolution is facilitated by the genetic aberrations that caused its malignancy as well as the extracellular environment surrounding the tumor, the tumor microenvironment.

Tumor Microenvironment and Acidosis

The tumor microenvironment consists of several cell types (cancer cells and stromal cells), chemical signals, and extracellular matrix. There is extreme variation established in the tumor microenvironment in comparison to normal tissue. One important reason for this difference is altered tumor cell metabolism. As previously mentioned, the tumor microenvironment is characteristically acidic as a result of deregulated cancer cell metabolism, poor blood perfusion, and hypoxia (83, 84, and 85) (Diagram 1). Acidosis has been reported to influence gene transcription and both facilitate and inhibit metastatic progression (18 and 36). It

is well known that hypoxia may cause acidosis, but they may also occur independently of one another (18). It has been reported that acute hypoxia and acidosis may facilitate the expression of distinct gene sets in human mammalian epithelial cells (18). Hypoxia is reported to stimulate the transcription of glycolytic genes such as lactate dehydrogenase (18). Acidosis may repress glycolytic gene transcription stimulated by hypoxia and kindle the activity of several genes that are associated with the citric acid cycle and electron transport (18). Moreover, it has been determined that acidosis may also inhibit protein kinase B activity in prostate cancer, which is crucial for glucose uptake, cell survival, and proliferation as well as cell motility (18).

There are several effects that acidosis may have on metastatic development. In this section two types of effects will be described. The first is the acute acidosis related effects and the second is the chronic acidosis related effects. Acute acidosis related effects have been known to cause cell death and the inhibition of metastatic progression (18 and 49). In a report previously mentioned were the specific gene sets that were activated in human mammalian epithelial cells following acute exposure to acidosis (18). The specific gene expression response to acute acidosis was then used in the same study to create a gene signature profile reflecting an acidosis gene expression response (18). Four breast cancer datasets were studied and next used to generate Kaplan-Meier survival curves (18). The gene expression response to acute acidosis in human breast cancers correlated with a favorable prognosis in clinical outcomes (18).

The chronic acidosis related effects have been portrayed as a metastatic facilitator due to its ability to facilitate the secretion of proteases such as cathepsin B from tumor cells, which results in the remodeling and degradation of the extracellular matrix (63 and 90). Degradation of extracellular matrix proteins and the basement membrane surrounding a tumor could hypothetically ease the movement of migratory cancer cells through tissue and into the blood

stream or local lymph nodes. Furthermore, during chronic acidosis cancer cells may have the increased ability to adapt to acidic conditions in comparison to normal cells (49). This may confer a survival advantage in tumor cells and by reducing the volume of normal cells surrounding a tumor the area available for tumor growth increases. As you can see the constructive and adverse effects of acidosis on the evolution of metastatic development are extremely complex and have become an important aspect of study in tumor biology and metastasis.

Invasion and Metastasis

As previously mentioned, one of the hallmarks of cancer is invasion and metastasis. In a clinical setting, one of the frequent signs of solid tumor invasion and metastasis is the presence of cancer cells in the sentinel lymph nodes, the lymph nodes closest to the tumor itself (55). However, the disseminated cancer cells found in the sentinel lymph nodes are not usually responsible for metastasis at distant sites (16). The majority of cancer cells that seed new foci at distant sites will have done so through a hematogenous metastasis (16). Hematogenous metastasis may occur as a result of clonal evolution and a cumulative alteration in gene expression. As the cell population within the primary tumor evolves, subpopulations may develop a migratory and invasive phenotype. To develop this phenotype, these cells may experience what is known as epithelial mesenchymal transition (82 and 93). Epithelial mesenchymal transition is a process that occurs during embryogenesis and primary tumor development. It is a transdifferentiation program that employs several transcription factors to directly, e.g. Snail, Zeb, E47, and KLF8, or indirectly, e.g. Twist, Goosecoid, E2.2, and FoxC2, inhibit the transcription of epithelial cadherin (6, 78, and 82). Transcription factors that stimulate epithelial mesenchymal transition control the expression of genes that may aid in the process of

cell survival, e.g. cadherin 2 (6, 78, and 82). The alteration in cell behavior that takes place following this process assists in the development of a migratory cell phenotype and may further primary tumor local, regional, and distant metastasis (78). Following the initial invasion of cancer cells from the primary tumor through the extracellular matrix they may be free to enter the blood stream and invade the body. As many primary tumor cells may enter the blood stream, only 0.01% of them will make it to a distant tissue and form a metastatic lesion (47).

The blood stream is a harsh environment for a circulating cancer cell because of host defenses such as the immune system and further because of its detachment from the extracellular matrix. The sooner a circulating cancer cell attaches to a distant tissue the better chance it may have for survival. Once in circulation cancer cells use a variety of ligands and receptors to attach to a distant surface. Known ligands used by circulating cancer cells are CD62 antigen-like family member E, Cadherin 2, and intracellular adhesion molecule 1 (8, 26, and 73). Similar to leukocytes responding to inflammation, extravasation from the blood stream into tissue has three distinct steps. The first step is the loose attachment of the cell to the surface of the endothelium. This attachment may be due to various chemical attractants; e.g. chemokine 12 attracts circulating cancer cells that express chemokine receptor type 4 to the bone marrow (8 and 43). Chemokine receptor type 4 is highly expressed in several cancers including breast, colon, and prostate (8 and 43). Following loose attachment, blood flow moves the cell along the surface giving it a characteristic rolling appearance (73). Soon after the cell has attached it would need to tightly adhere to the surface (73). The last two steps are cell spreading and diapedesis (73). In these steps the cancer cell actively spreads out and migrates into the tissue.

Cell Spreading

Cell spreading will be discussed in the following section because of its importance in the survival of circulating cancer cells after their attachment onto a distant tissue. Cell spreading is essential during normal embryonic development and physiological function. It is necessary for many processes such as embryogenesis, wound healing, tissue remodeling, and immune surveillance (60, 73, and 86). The commencement of cell attachment and spreading is accomplished by an initial clustering of integrins on the surface of the cell after contact with a suitable substrate (69) (Diagram 2). The regions where integrins cluster and the actin cytoskeleton is anchored to a substrate are labeled focal adhesions. Focal adhesions are sites where several proteins aggregate, e.g, talin, paxillin, focal adhesion kinase (FAK), etc., and subsequently stimulate intracellular signaling cascades that may facilitate cell survival, proliferation, and movement (Diagram 2). The activation of integrins following cell attachment to the substratum stimulates the intracellular attraction of SRC kinase to the site of clustering (69). The attraction of SRC kinase allows for the interaction of the SRC homology domain of SRC kinase with focal adhesion kinase's autophosphorylation site tyrosine 397 (53, 56, and 69). Focal adhesion kinase is a particularly important focal adhesion protein that contributes to several cell processes, e.g. cell proliferation, survival, invasion, and migration (33, 34, 53, 69, and 71). The activation of focal adhesion kinase leads to the subsequent activation of other focal adhesion proteins by SRC kinase and FAK such as P130Cas and paxillin as well as other sites located on focal adhesion kinase itself (53 and 69). These phospho-tyrosine residues act as docking sites for intracellular signaling proteins. Phospho-tyrosine residues can also stimulate the activity of Rho and Rac Guanine nucleotide Exchange Factors (GEFs) and GTPase Activating Proteins (GAPs) thus increasing or reducing their activity (45, 53, 59, 76, 77, 98 and

99). Consequently, an alteration in the activity of the Rho family of small GTPases may have numerous effects on cell morphology and function (Diagram 3).

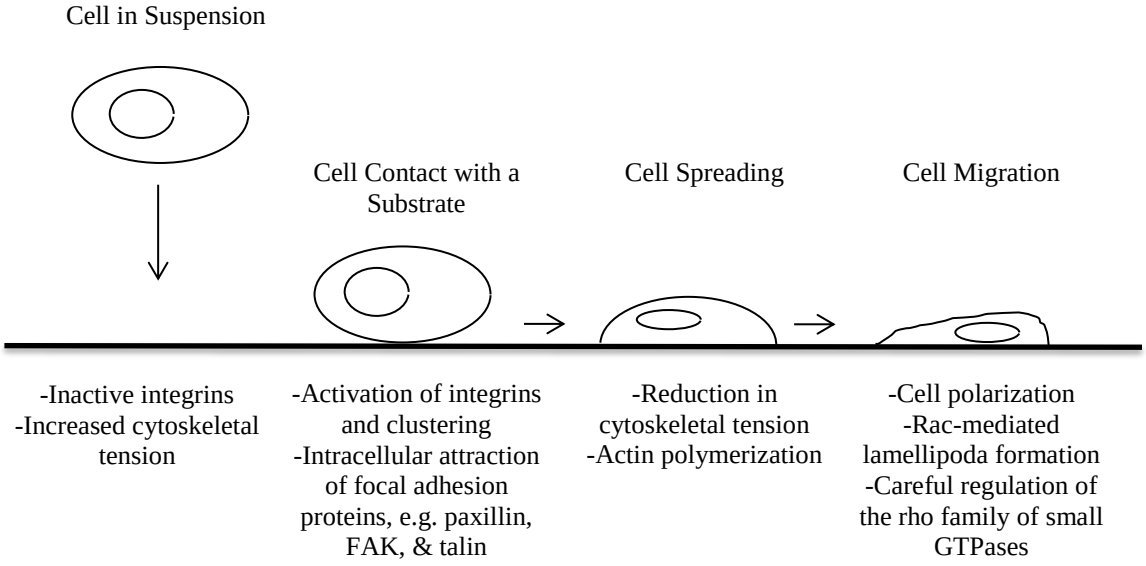

Diagram 2. Normal Cell Spreading

There are several members in the Rho family of small GTPases and their regulation is extremely important for cell attachment, spreading, and migration (Diagram 3). It has been well established that Rac activation is responsible for an accumulation of actin in the peripheral regions of the cell. This accumulation of actin is followed by the formation of membrane ruffles and lamellipodia that will aid the cell in polarization and mesenchymal-like migration (64). Lively regions such as membrane ruffles and the lamellipodia are composed of highly dynamic focal adhesions that exhibit a high turnover rate. Turnover rate refers to the time it takes to form and breakdown focal adhesions. The high turnover rate that focal adhesions have in these specific areas contributes to efficient membrane ruffling, cell spreading, and migration (57). Rac

activation is also vital for cell spreading due to its ability to facilitate the uncapping of microfilament capping proteins such as gelsolin (20). Gelsolin removal allows for actin polymerization that will ultimately push on the membrane to spread the cell (20). As activation of Rac is extremely important for cell spreading, an additional family member of the Rho family of small GTPases, Rho, is important for cell spreading as well. It has been established in various reports that aberrant activation of Rho will delay the early stages of cell spreading due to an increase in actomyosin contractile forces and cytoskeletal tension (5 and 86). For example, during the initial stages of cell spreading, P190RhoGAP may hydrolyze Rho-GTP to Rho-GDP to diminish actomyosin contractile forces (5). The deactivation of Rho and reduced cytoskeletal tension allows rac-mediated cell spreading without hinderance from myosin activity (Diagram 3). When Rho and Rac activation levels are not correctly regulated cell spreading will be delayed and membrane protrusions may be reduced. Moreover, there is a reported reciprocal relationship that Rho and Rac have (12). Several studies report Rac activation as a potential indirect activator of numerous Rho-GAPs and the regulation of this reciprocal relationship is essential for determining cell morphology and rate of cell spreading (5 and 65). Lastly, cell spreading is vital for the survival and progression of circulating cancer cells and therefore it is a potential target in cancer therapy (15, 60, 68, and 98).

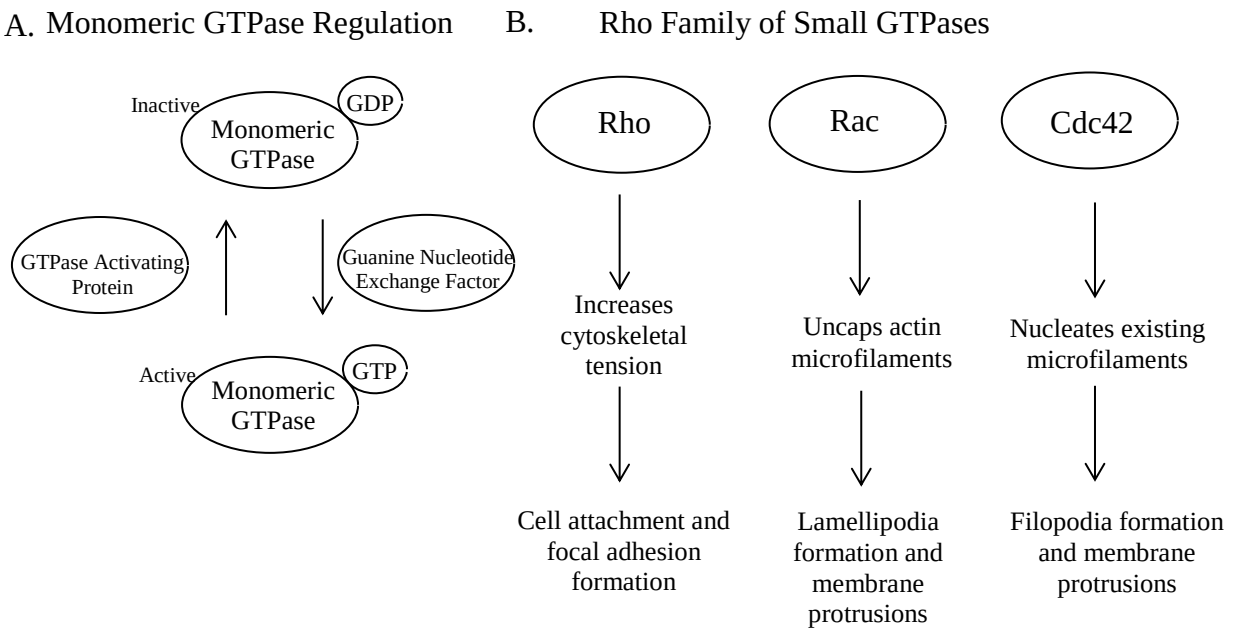

Diagram 3. The Regulation of the Rho Family of Small GTPases and their Function.

Increasing the cells contact with a substrate is important for the activation of intracellular signaling, which may lead to cell survival, growth, and division (33, 34, 35, 53, 69, and 71). It has been established that the amount of cell contact with a substrate is directly correlated with apoptotic index, which specifies that a reduction in surface area contact may increase apoptosis in cells (60). Furthermore, the adherence state of cancer cells to extracellular matrix proteins correlates with increased therapeutic resistance, reviewed in (92). This presents a niche for drugs that reduce cell spreading and subsequently allow for the sensitization towards other chemo-therapeutic agents. Of the several cancer therapies directed at cell spreading, there are current studies that are directed towards cell spreading for the sensitization to TNF-related apoptosis-inducing ligand (TRAIL) directed treatments (54). TRAIL is a molecule that is targeted for the clearance of circulating cancer cells from the blood stream by natural killer cells. TRAIL's

binding to TRAIL receptors induces apoptosis and by reducing cell spreading before treatment, its therapy has been sensitized (54).

In addition to TRAIL therapy sensitization there are also drugs that are aimed at receptor and non-receptor tyrosine kinases. Non-receptor and receptor tyrosine kinases such as focal adhesion kinase, SRC, and epidermal growth factor receptor have been reported overexpressed in several cancers (3 and 7). Cancers that are known to overexpress receptor tyrosine kinases have been recently targeted. Many treatments have already found their way to clinical trials and a select few such as Erlotinib against non-small cell lung cancer; Sutent against kidney cancer; and Sorafenib against solid tumors such as melanomas and carcinomas have already been marketed (4). Targeting over-expressed receptors that may control the rate of cancer cell spreading may reduce the possibility of a macrometastatic cancer growth. To be more specific, targeting focal adhesion kinase and SRC receptor tyrosine kinases in particular may reduce cell spreading and are advantageous for later stage cancer therapies (4). Cancer therapies directed toward cell spreading appear to be very promising and may leave a window open for sensitization towards many other chemical therapies.

Cell Migration

In this study we investigate the dynamics of cell migration on a two-dimensional substrate. In vitro cell migration will be described and will be elaborated upon due to the correlation between in vitro cell migration and the virulence of cancer cells in vivo. Cell migration is a highly dynamic process that is necessary for normal embryonic development, immune function, and several other physiological processes. Cancer research in particular has placed an emphasis on the study of cell migration. As previously mentioned, cell migration

plays an important role in facilitating the dissemination of cancer cells into other areas of the body such as the blood stream and lymph system. There are several methods of cell migration such as single cell migration in the case of leukocytes, fibroblasts, neuronal cells, and lymphocytes or group movement commonly seen for example in epithelial cells and endothelial cells (62).

In vitro, single cell migration on a two-dimensional substrate may be divided into four mechanically separate steps: lamellipodia extension, formation of new adhesions, cell body contraction, and lastly trailing edge detachment (42). Cell migration is mediated by several intracellular responses to extracellular cues. Filopodia are membrane protrusions that extend from the cell body in order to sense extracellular cues and aid the cell during migration on a two-dimensional substrate (50). The main activator of filopodia growth is the small GTPase Cdc42 (50). Cdc42 is a member of the Rho family of small GTPases and is reportedly activated by several proteins such as paxillin and P21 activated kinase 3 (11 and 50). As filopodia sense extracellular cues for directional migration other proteins that belong to the Rho family of small GTPases also do their part to insure efficient cell migration. Rac as mentioned previously is a member of the Rho family of small GTPases and its activation is not only crucial for cell spreading but cell migration as well. The uncapping of actin microfilaments by Rac activation permits efficient actin polymerization and treadmilling. This will also facilitate the formation of a large broad shaped structure at the leading edge of the cell labeled the lamellipodia. To efficiently migrate, the cell must form new focal contacts quickly in the leading edge of the lamellipodia and it must also disassemble mature focal adhesions in the rear to continue. To provide the leading edge with ease of movement this area has an increased rate of focal adhesion turnover. After polarizing, extending its leading edge, and forming new focal adhesions the cell

must then use actomyosin contractility to contract itself in order to move across the surface. The process of actomyosin contractility may be activated by Rho and subsequently the interaction between myosin II and actin microfilaments (86). Actomyosin contractility can be visualized underneath the microscope by using Rhodamine phalloidin, a fluorescence labeled toxin that binds to microfilaments. Actin stress fibers may be visible if this step is occurring (3). Finally, to complete the migration process, the trailing edge of the cell must then undergo focal adhesion disassembly to allow the cell to move forward (14, 30, and 72).

G-Protein Coupled Receptors

G-protein coupled receptors (GPCR's) are the largest family of cell surface membrane receptors (24). Humans contain over 700 different types of GPCR's and mice use over 1000 just for smell (1). These receptors span the membrane seven times and specifically activate heterotrimeric G-proteins that may activate or inhibit several intracellular signaling pathways. GPCR's have a wide variety of ligands such as peptides, hormones, lipids, photons, ions, and nucleotides (66). Furthermore, GPCR's are an extremely sought after pharmaceutical target and half of all drugs in the market today target them (19 and 24).

When a ligand binds a GPCR and activates it the receptor undergoes a conformational change and stimulates the activity of a heterotrimeric G-protein (Diagram 4). The cytoplasmic G-protein is attached to the plasma membrane where it connects the receptor to an enzyme or an ion channel. There are three protein subunits that make up a G-protein: alpha, beta, and gamma (1) (Diagram 4). When the receptor is inactive the alpha subunit is bound to Guanosine Diphosphate (GDP), but when activated, the alpha subunit will release GDP. When GDP is released the G-protein will alter its conformation and permit the binding of Guanosine

Triphosphate (GTP), which activates the alpha subunit of the G-protein and allows for it to disassociate from the beta and gamma subunits to perform its function (Diagram 4). There are four families that make up the heterotrimeric G-proteins. They are classified by the relatedness of the amino acid sequences in their alpha subunit (1). Discussed in this study in family one is the G_s pathway, in family two is the G_i pathway, in family three is the G_q pathway, and finally the most important pathway in this report is in family four, the $G_{12/13}$ pathway (Table 1).

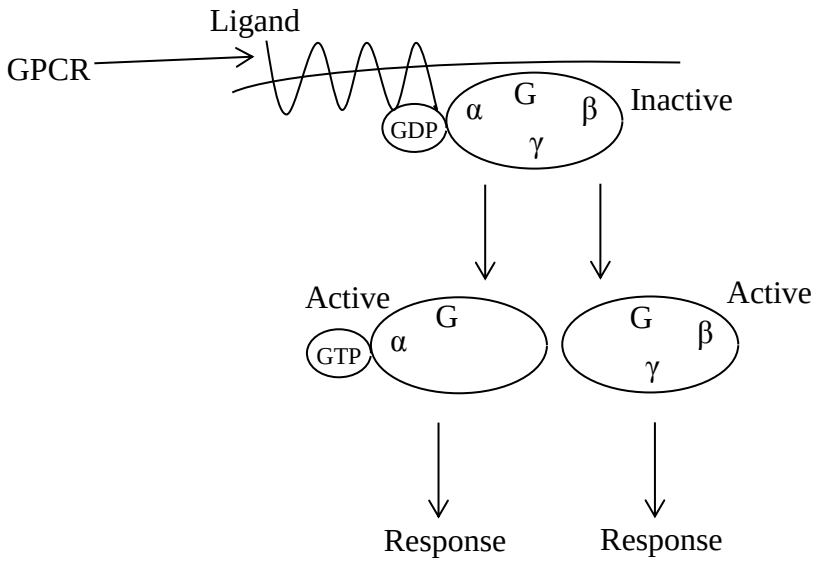

Diagram 4. Activation of a Heterotrimeric G-protein.

To begin a light introduction to G-protein signaling pathways, GPCR's that are coupled to the G_s G-protein stimulates the activation of adenylyl cyclase (AC), a multi-pass transmembrane protein that stimulates cyclic adenosine monophosphate (cAMP) production. cAMP is a small molecule in the cell that serves various purposes (Table 1) (1). Alternatively,

when the G_i G-protein is activated it inhibits the activation of adenylyl cyclase (AC), therefore reducing cAMP levels.

The G_q G-protein activates phospholipase C-β (PLC-β). Activation of PLC- β leads to the cleavage of phosphotidylinositol 4, 5-bisphosphate into Inositol trisphosphate (IP_3), which stimulates the release of calcium from IP_3-gated calcium channels in the endoplasmic reticulum, and diacylglycerol (1). Diacylglycerol activates protein kinase C and translocates it from the cytosol to the intracellular portion of the plasma membrane where it phosphorylates a wide range of target proteins (1). A large increase of cytosolic calcium targets receptors such as Ca^{2+}/calmodulin-dependent protein kinases and may lead to the phosphorylation of a number of regulatory proteins such as myosin light chain kinase (MLCK) (1). Calcium also accumulates in the mitochondria after its release into the cytosol; this accumulation has been reported to control the rate of energy production in the cell (38).

The $G_{12/13}$ G-protein may be activated in response to various ligands. Its activation may be of particular interest when studying cell attachment, spreading, and migration. Downstream of $G_{12/13}$ is the activation of P115 Rho-Guanine nucleotide Exchange Factor (GEF) and subsequently Rho, which regulates the actin cytoskeleton (39). This facilitates the exertion of actomyosin contractile forces and increases cytoskeletal tension (3). $G_{12/13}$ G-protein downstream signaling pathways are investigated throughout this report and are responsible for the majority of the effects seen in B16/GPR4 cells following GPR4 activation.

Table 1. G-protein signaling pathways

G-Protein	**G_s**	**G_i**	**G_q**	**$G_{12/13}$**
Ligands	Proton, Cholic Acid, Dopamine	CCL13, CXCL1	Proton, Adrenaline, Acetylcholine	Proton, LPA
Receptors	GPR4, GPBA, D_1 Receptor	CCR1, CXCR1	GPR4, Alpha 1 Adrenergic Receptor, M_1 Receptor	GPR4, LPA Receptor
Primary Response	Stimulates Adenylyl Cyclase activity.	Inhibits adenylyl cyclase activity.	Stimulates PLC and results in the production of IP3 and DAG from PIP_2.	Activates P115 Rho-GEF.
Biochemical Response	Increases cAMP production and activates PKA.	Reduces cAMP production.	Stimulates Ca^{2+} release and the PKC pathway.	P115 Rho-GEF exchanges GDP for GTP rendering Rho active.
Biological Response	Glycogen breakdown, bone resporption, water resorption, triglyceride breakdown, cortisol secretion, and progesterone secretion, etc.	Cell proliferation, apoptosis, metabolic changes, etc.	Phosphorylation events, gene transcription, energy production	Actin stress fiber formation and cell anchorage. (cytoskeletal tension)

Proton Sensing G-Protein Coupled Receptors

There are a number of ligands that may bind a G-protein coupled receptor to stimulate a response by the heterotrimeric G-proteins (66) (Table 1). The main ligand that will be focused on throughout this project is the proton. The proton has been reported to activate a GPCR appropriately labeled the proton-sensing G-protein coupled receptor (67). Several extracellular histidine residues are responsible for its proton sensing abilities (67). This type of receptor can function in several locations throughout the body such as the kidneys, endothelial cells, lungs, and other regions that may require a delicate pH balance (74 and 94). When the proton sensing G-protein coupled receptor is stimulated by an increase in proton concentration, it elicits a proper response by the cell. In the family of proton-sensing G-protein coupled receptors, there are several members such as GPR4, TDAG8, G2A, and OGR1 (67). The only receptor that will be focused on in this report is GPR4 and its effects on B16F10 melanoma cell spreading and migration following overexpression and activation.

GPR4 signaling has not been fully elucidated but the results established so far have promise in cancer research. GPR4 has been known to activate several heterotrimeric G-proteins such as G_s, G_q, and $G_{12/13}$ (15, 46, and 94). Previous studies with B16F10 melanoma cells that have been genetically engineered to express GPR4 at a high level have demonstrated that cell migration in vitro is inhibited at pH 6.4 and pulmonary metastasis post tail vein injections in mice is reduced (15). However, the effects of GPR4 overexpression on cell attachment, spreading, and focal adhesion dynamics have not yet been investigated. This report examines the G-protein signaling pathways responsible for delayed cell spreading and migration found in B16F10 melanoma cells genetically modified to express GPR4 at a high level, namely B16/GPR4 cells.

Chapter 2: Materials and Methods:

Cell Lines

B16F10 melanoma cells were used throughout this study to characterize the effect of the activation of GPR4 on cell spreading and migration. All cell lines were cultured in Dulbecco's Modified Eagle Medium (DMEM) supplemented with 10% fetal bovine serum (FBS) in a tissue culture incubator set at 5% CO_2 and 37° C. During experimental procedures DMEM supplemented with 10% FBS was buffered to pH 6.4, 7.4, or 8.4 using 7.5 mM 4-(2-Hydroxyethyl)-1-piperazineethanesulfonic acid from Fisher Scientific (Fair lawn, N.J.), 7.5 mM N-(2-Hydroxyethyl)-piperazine-N-N-3-propanesulfonic acid from Sigma-Aldrich (St. Louis, MO), and 7.5 mM 2-(4-Morpholino)-ethanesulfonic acid from Fisher Scientific (Fair lawn, N.J.), (known collectively as HEM). 5N Hydrochloric Acid and Sodium Hydroxide were used to buffer media to the desired pH. Cells grown in normal cell culture were grown to no more than 90% confluence, had a passage number below 10, and were 95% viable. Cells that were harvested for experiments were grown to no more than 70-80% confluence, had a passage number below 10, and were 95% viable.

B16/Vector and B16/GPR4 cells were previously generated by other investigators from Dr. Yang's laboratory (15). B16F10/Vector cells represent a B16F10 melanoma cell line that was transduced with an empty vector, MSCV-IRES-GFP, as the control (15). The B16/Vector cells had only a minor endogenous expression level of GPR4 (Figure 1). To create the B16/GPR4 cell line, GPR4 cDNA was cloned into a MSCV-IRES-GFP retroviral vector as previously described (95), and was transduced into B16F10 melanoma cells for a stable GPR4 overexpressing cell line as previously described (15). The resultant MSCV-huGPR4-IRES-GFP vector infected cells were sorted by fluorescence-activated cell-sorter for EGFP positive cells

(15). In addition, B16/Vector and B16/GPR4 cells were pooled and not clonal. This ruled out the possibility of any gene insertion-related phenomenon that could conceivably alter the results. The overexpression of GPR4 in B16/GPR4 cells was confirmed previously by running RT-PCR due to the unavailability of an antibody directed towards GPR4 (15) (Figure 1). In the RT-PCR 35 cycles were run at an annealing temperature of 58°C (15) (Figure 1).

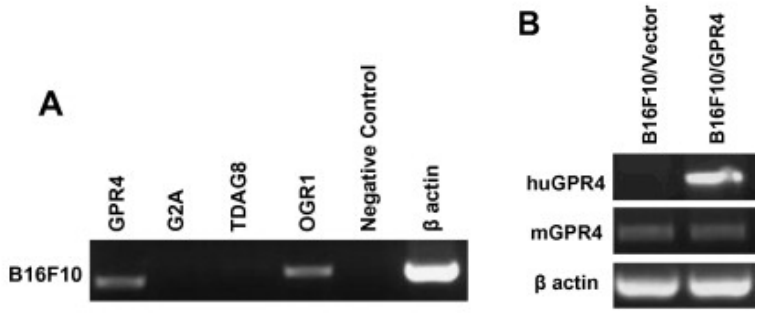

Figure 1. RT-PCR of B16F10, B16Vector, and B16/GPR4 Cells. (A) RT-PCR previously completed to examine the endogenous expression of GPR4 in B16F10 cells (15). (B) RT-PCR to confirm the overexpression of the huGPR4 construct in B16/GPR4 cells.

The constructs, GRK-RGS PQCXIP, P115-RGS PQCXIP, and control PQCXIP used in this study was generated by previous lab members (95). In this report, to generate the B16/GPR4 $G_{12/13}$- and G_q- ($G_{12/13}$ and G_q signaling deficient) cell lines, previously GRK2-RGS and P115 Rho-GEF RGS constructs were subcloned into the PQCXIP retroviral vector (13, 39, and 95). The PQCXIP retroviral vector was then transduced into the B16/GPR4 cells using the procedure found in (95). B16/GPR4 cells following transduction were selected for with 2µg/mL puromycin for three days or until the control without resistance was completely killed.

Tissue Culture Plate Attachment Assay

Cells were detached using 0.25% Trypsin-EDTA from GIBCO® by Life Technologies™. Next, $5x10^4$ cells were resuspended in DMEM supplemented with 10% FBS buffered to pH 6.4, 7.4, or 8.4 in a Becton Dickinson Multiwell™ 24-well tissue culture plate. Chemical treatments were administered at the time of cell plating. Subsequently plates were positioned into an incubator set at 37°C and 5% CO_2 for one hour. The plates were then placed under the EVOS®*fl* Digital Inverted Microscope and 10 pictures were taken at 200X total magnification in various non-specific and random areas of each well (1-4 wells). Furthermore, to confirm cell attachment to the plate, each plate was tilted to the side to observe cell movement. The movement of unattached cells in media was extremely low in all treatment groups after one hour of incubation. In addition, the unattached cells were easily visible and were avoided when taking pictures.

To quantify the results of cell spreading, every cell in each field of view (FOV) was classified as round, spread, or migrating based on its morphology and then counted using Adobe Photoshop's counting tool (Diagram 5). A round cell was characterized by absolutely no membrane protrusions, a spread cell was characterized by any cell with membrane protrusions, and a migrating cell was characterized by any polarized cell that represented the characteristics of a migrating cell, e.g. polarized, lamellipodia, and tail (Diagram 5). To acquire the percentages of the diverse morphological features of each cell line the number of round, spread, or migrating cells in each field of view was divided by the total number of cells in each field of view (30-40 cells/FOV) (1-4 wells). The average round, spread, or migrating cell percentages were represented using a bar graph and tested for statistical significance using the unpaired t-test.

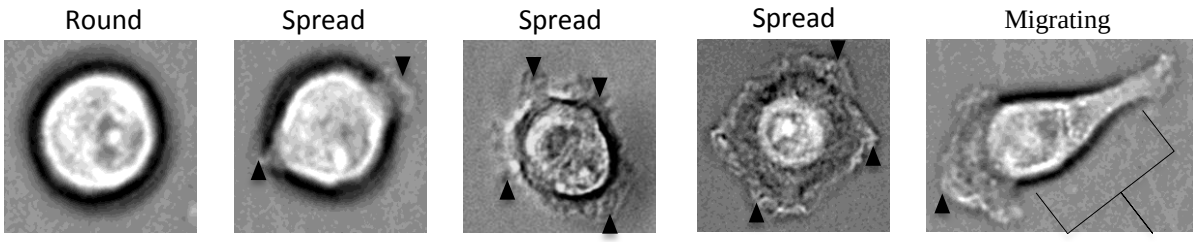

Diagram 5. Cell Attachment Assay Characterization.

Matrigel Attachment Assay

Matrigel was thawed on ice for one hour previous to its application to tissue culture plates. After the matrigel was thawed, 48 µl's of matrigel was added to each well in a Becton Dickinson Multiwell™ 96-well tissue culture plate and placed into the incubator set at 37° C and 5% CO_2 for 30 minutes. After the matrigel solidified into a gel, $1x10^4$ B16/Vector, B16/GPR4, B16/GPR4 $G_{12/13-}$, B16/GPR4 G_{q-}, or B16/GPR4 PQCXIP cells from cell culture were plated onto matrigel in 2mL DMEM supplemented with 10% FBS buffered to pH 6.4, 7.4, or 8.4 and subsequently placed into the incubator set at 37° C and 5% CO_2 for 1 hour. Plates were then removed and 5 pictures were taken at 200X total magnification of each well (2 Wells) using the EVOS®*fl* Digital Inverted Microscope. The same quantification method used in the tissue culture plate attachment assays were used to quantify the morphological features of B16F10 cells after attaching and spreading onto matrigel.

Actin Staining

To start, $2x10^4$ cells were seeded in DMEM supplemented with 1% FBS on top of a 15 mm round FISHER brand glass coverslip inside each well of a 24 well tissue culture plate. The

cells were allowed to grow for 24 hours. The media was aspirated after 24 hours and DMEM without FBS was added to each well. The plates were incubated for 48 hours and the existing media was aspirated. Subsequently, DMEM without FBS buffered to pH 6.4 or 7.4 was added to the well and the plates were incubated in a sealed chamber for 1 hour at 37° C and 5% CO_2. Next, the media was aspirated and the wells were washed once with Dulbecco's Phosphate-Buffered Saline (DPBS) (GIBCO®). Cells were then fixed with a 4% paraformaldehyde solution for 15 minutes at room temperature and washed with DPBS. Next, 0.1% Triton-X permeabilization buffer (0.1% Triton-X in DPBS) was added to each well and incubated at room temperature for 5 minutes then washed with DPBS. A working stock solution of 100nM Rhodamine phalloidin in DPBS was added to each well and the tissue culture plate was wrapped in tin foil. It was then incubated for 30 minutes at room temperature. Following incubation, the media was aspirated, the well was washed three times with DPBS, and the glass coverslips were flipped over onto a microscope slide with one drop of VECTASHIELD® Mounting Medium for fluorescence with DAPI. The glass coverslip was sealed using clear nail polish and pictures were taken with a fluorescence microscope and a digital camera at 400X total magnification (Nikon).

Phospho-Paxillin (Y118), Total Paxillin, and Phospho-Focal Adhesion Kinase (Y397) Immunocytochemistry (ICC)

To begin, cells were detached with 0.25% Trypsin EDTA. Next, $2.5x10^5$ cells were resuspended in DMEM supplemented with 10% FBS buffered to pH 6.4, 7.4, or 8.4 on a 15 mm round FISHER brand glass coverslip inside of a 24 well Becton Dickinson Multiwell™ tissue culture plate. The cells were then placed into an incubator set at 37° C and 5% CO_2 for one hour to allow attachment. The media was aspirated and the wells washed twice with DPBS. The cells were fixed for 15 minutes with 4% paraformaldehyde. Following fixation, the cells were washed

three times with DPBS and .1% triton-X permeabilization buffer was added for four minutes and aspirated. Using a 1:20 dilution goat serum in PBS-T (0.1% Tween-20 in 10X DPBS), the glass coverslips were blocked for one hour at room temperature. The blocking solution was then aspirated and the primary antibody phospho-paxillin (Y118) from Cell Signaling Technology®, total paxillin from Santa Cruz Biotechnology Inc., or phospho-focal adhesion kinase (Y397) from Cell Signaling Technology® was diluted in the blocking serum 1:50 or 1:100 and added into each well. It was then placed on the shaker in the 4° C freezer overnight. Following aspiration of the primary antibody solution the secondary antibody goat anti-rabbit Rhodamine Red™ in goat serum + PBST at a 1:200 dilution was added to the well for one hour at room temperature. The secondary antibody solution was aspirated and the glass coverslips were washed five times. Next, the glass coverslips were flipped over onto a microscope slide with a drop of VECTASHIELD® Mounting Medium for fluorescence with DAPI. The glass coverslips were sealed with clear nail polish and observed under 1000X total magnification. To clearly display the data collected from the immunocytochemistry of phospho-paxillin (Y118) and phospho-FAK (Y397) a 3-D surface plot was created using Image-J software and further represented using thermal LUT imagery. Due to the unequal exposure values between samples, the 3-D thermal LUT surface plot is not used to compare the intensity between samples, but only the distribution of the signal.

Time-Lapse Cell Culture Wound Closure Assay

Cells were seeded at $1x10^6$ cells per well in a Becton Dickinson Multiwell™ six well tissue culture plate. The cells were allowed to attach and grow to 100% confluence over a 24 hour period in DMEM supplemented with 10% FBS. Using the tip of a pipette a wound was made vertically; the existing media and debris were aspirated and then washed once with DPBS.

Next, DMEM supplemented with 10% FBS buffered to pH 6.4, 7.4, or 8.4 was added to the well. The EVOS®*fl* Digital Inverted Microscope was used to run a 16-hour time-lapse cell culture wound closure assay in a controlled chamber set at 37° C and 5% CO_2. Pictures were taken every 5 minutes over a 16-hour time period at 100X total magnification to generate 193 pictures. After the images were saved into a file, they were imported into the Image-J program and a video was created. To quantify wound closure in every cell line, the cell culture wound closure assay was performed in 6 to13 wells of a 96 well plate. A picture was taken after the wound was initially made and following incubation, using a scale bar, the distance of wound closure was measured and divided by the number of hours incubated to get the velocity in which the wound closed. The average distance of wound closure is represented in a bar graph including error bars that represent standard error. The unpaired t-test was used to test for significance.

The analysis of individual B16F10 cells during the cell culture wound closure assay was completed by viewing the time-lapse video originally created by Image-J software. Cells that were clearly extending their leading edge and migrating individually were selected for viewing. Pictures were cropped and zoomed in to closely visualize cell migration dynamics.

Phospho-Paxillin (Y118) and Total Paxillin Immunocytochemistry of Migrating B16/Vector and B16/GPR4 Cells

Cells were seeded at $1x10^3$ cells per well in a Thermo Fischer Scientific, Eight-Well Lab-Tek II Chamber Slide with DMEM supplemented with 10% FBS and buffered to pH 6.4 or 7.4. Next, cells were incubated for 24 hours at 37° C and 5% CO_2. Subsequently, the media was aspirated and every well was washed once with DPBS. Next, 4% paraformaldehyde was added to each well for cell fixation and incubated at room temperature for 10 minutes. To permeabilize

cells, .1% Triton-X diluted in DPBS was added to each well, incubated at room temperature for 4 minutes, and aspirated. Each well was washed once with DPBS and aspirated. Using a 1:20 dilution goat serum in PBS-T (0.1% Tween-20 in 1X PBS), each well was blocked for one hour at room temperature. The blocking solution was aspirated and the primary antibody, Phospho-Paxillin (Y118) Rabbit mAb from Cell Signaling Technology® or total Paxillin from Santa Cruz Biotechnology, diluted in the blocking serum at a 1:50 or 1:100 dilution was added into each well. It was then placed on the shaker in the 4° C freezer overnight. Following aspiration of the primary antibody solution, the secondary antibody, goat anti-rabbit Rhodamine Red™ in goat serum + PBST at a 1:200 dilution was added to the well and incubated for one hour at room temperature. Next, each well was washed 5 times with DPBS and following aspiration the chamber separators were removed and a drop of anti-fade mounting medium with DAPI was placed on each well. Finally, a glass coverslip was placed on top and sealed using clear nail polish. Pictures were taken of cells that had a migrating morphology with a digital camera (Nikon) at 200X total magnification.

Statistical Analysis

Statistical analysis was performed using Prism software. The unpaired t-test was used to test for statistical significance in the one-hour cell attachment assay and the cell culture wound closure assay. Error bars represent standard error in all graphs. *** $P < .001$, ** $P < .01$, * $P < .05$, ns $P > .05$.

Chapter 3: Results

In the results section we describe the effects of GPR4 activation on B16/Vector and B16/GPR4 cell spreading, migration, and focal adhesion dynamics by using several in vitro assays. To begin, we investigated cell spreading using one-hour attachment assays to tissue culture plates, fibronectin, glass coverslips, and matrigel in DMEM supplemented with 10% FBS buffered to pH 6.4, 7.4, and 8.4. We then use these assays to determine potential G-protein pathways activated by GPR4. Furthermore, we use cell culture wound closure assays to investigate GPR4 overexpression during B16/Vector and B16/GPR4 cell migration. We also determine the rate of cell migration following the inhibition of the $G_{12/13}$ G-protein signaling pathway. Finally, we investigate focal adhesion dynamics following GPR4 activation in spreading and migrating B16/Vector and B16/GPR4 cells. In the following section, representative pictures of cell morphological changes will first be displayed and then the quantitative data will be presented.

GPR4 Activation Delays B16/GPR4 Cell Spreading

Initially, throughout normal cell culture, delayed B16/GPR4 cell spreading was observed. Due to the significance of cell spreading in cell survival and cancer metastasis, it was decided to explore what was causing the delay and if it was significant. To examine B16/GPR4 cell spreading several one-hour cell attachment assays on tissue culture plates in DMEM supplemented with 10% FBS buffered to pH 6.4, 7.4, and 8.4 were performed (Figure 2E-F). After plating B16/GPR4 and B16/Vector cells into tissue culture plates and performing one-hour attachment assays at pH 7.4, there was a small inhibition or delay in cell spreading (Figure 2C-D). At pH 6.4, however, B16/GPR4 cell spreading was markedly impaired in comparison to pH

7.4 and 8.4 treatment groups and when compared to all B16/Vector treatment groups (Figure 2B).

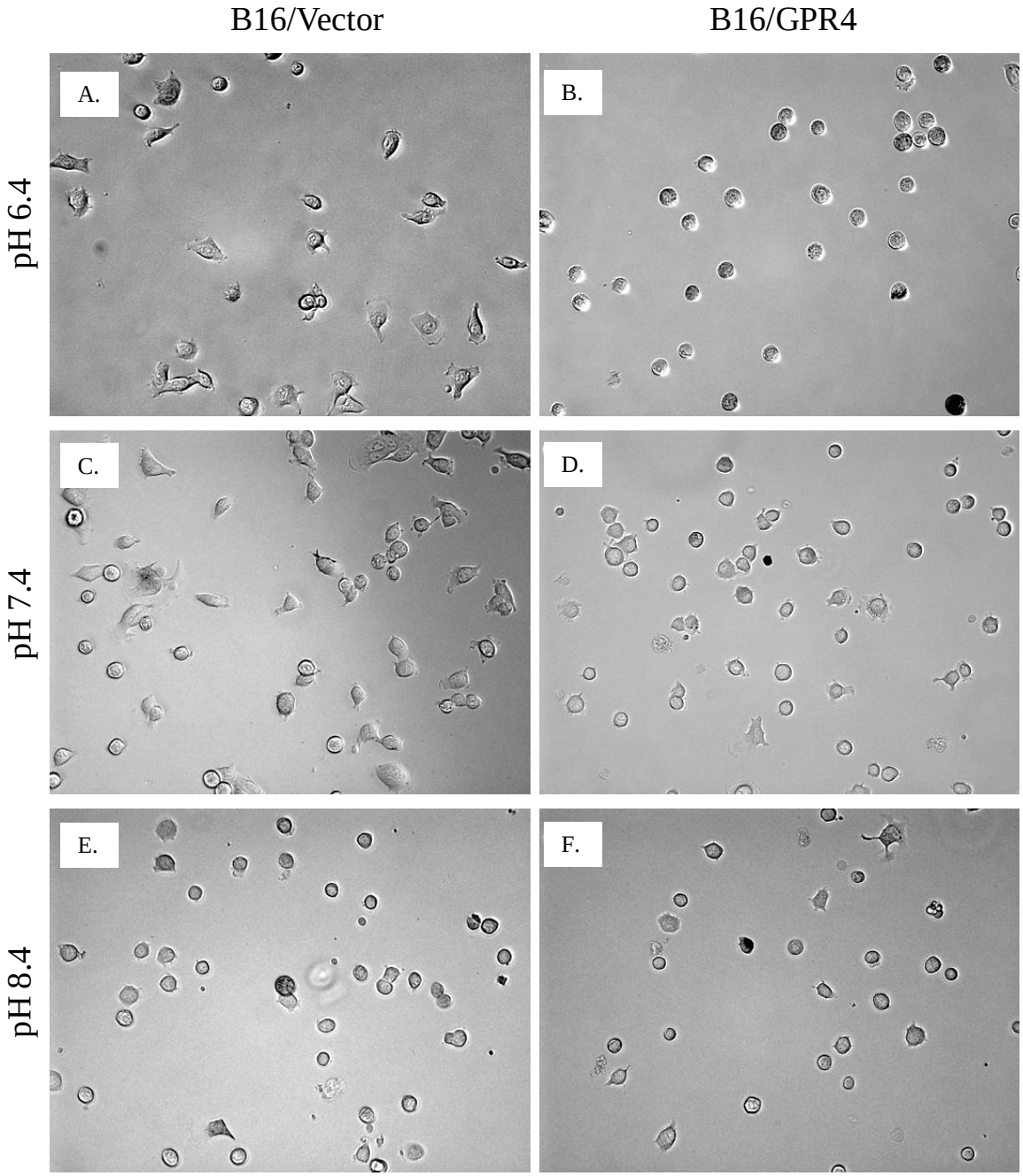

Figure 2. Representative Pictures of B16/Vector and B16/GPR4 Cell Spreading (A) and (B) B16/Vector and B16/GPR4 cell attachment and spreading at pH 6.4. (C) and (D) B16/Vector and B16/GPR4 cell attachment and spreading at pH 7.4. (E) and (F) B16/Vector and B16/GPR4 cell attachment and spreading at pH 8.4. Assay was repeated multiple times, e.g. Figure 3. (200X total magnification)

GPR4 Activation Significantly Delays B16/GPR4 Cell Spreading

To quantify the difference in cell spreading following the one-hour attachment assays, $5x10^4$ B16F10 melanoma cells were seeded into 24 well tissue culture plates with DMEM supplemented with 10% FBS buffered to pH 6.4, 7.4, or 8.4. Next, after one hour of incubation, 10 pictures of each well were taken (4 wells/treatment group) at 200X total magnification. Using the Adobe Photoshop's counting tool, the number of round, spread, and migrating cells were then counted (Diagram 5). Next, the number of round, spread, or migrating cells in each field of view (FOV) was divided by the total number of cells to obtain a percentage (30-40cells/FOV). B16/GPR4 cells at pH 6.4 exhibited 80% round cells on average compared to 33% at pH 7.4 signifying a significant pH-dependent delay in cell spreading (Figure 3A). Furthermore, 19% of B16/Vector cells at pH 6.4 were round, which demonstrates a significant cell line dependent delay in B16/GPR4 cell spreading (Figure 3A). The B16/Vector round cell percentage was only slightly significant between pH 6.4 and 7.4 treatment groups, which indicate that GPR4 activation in B16/GPR4 cells is responsible for delayed cell spreading (Figure 3A). Lastly, the migrating B16/Vector cell percentage was increased 10% at pH 6.4 (Figure 3C). This may possibly indicate a normal migratory cell response to acidosis without overexpression of GPR4.

To further investigate delayed cell spreading, B16/Vector and B16/GPR4 cells were plated and serum starved for two days. Next, cells were treated with DMEM without FBS buffered to pH 6.4 or 7.4 for one hour and stained with Rhodamine phalloidin. B16/GPR4 cells displayed high actin stress fiber development at pH 6.4 but not at pH 7.4 (Figure 3D). In contrast B16/Vector cells did not form actin stress fibers (Figure 3D). This indicates increased cytoskeletal tension in B16/GPR4 cells, which may delay the initial stages of cell spreading.

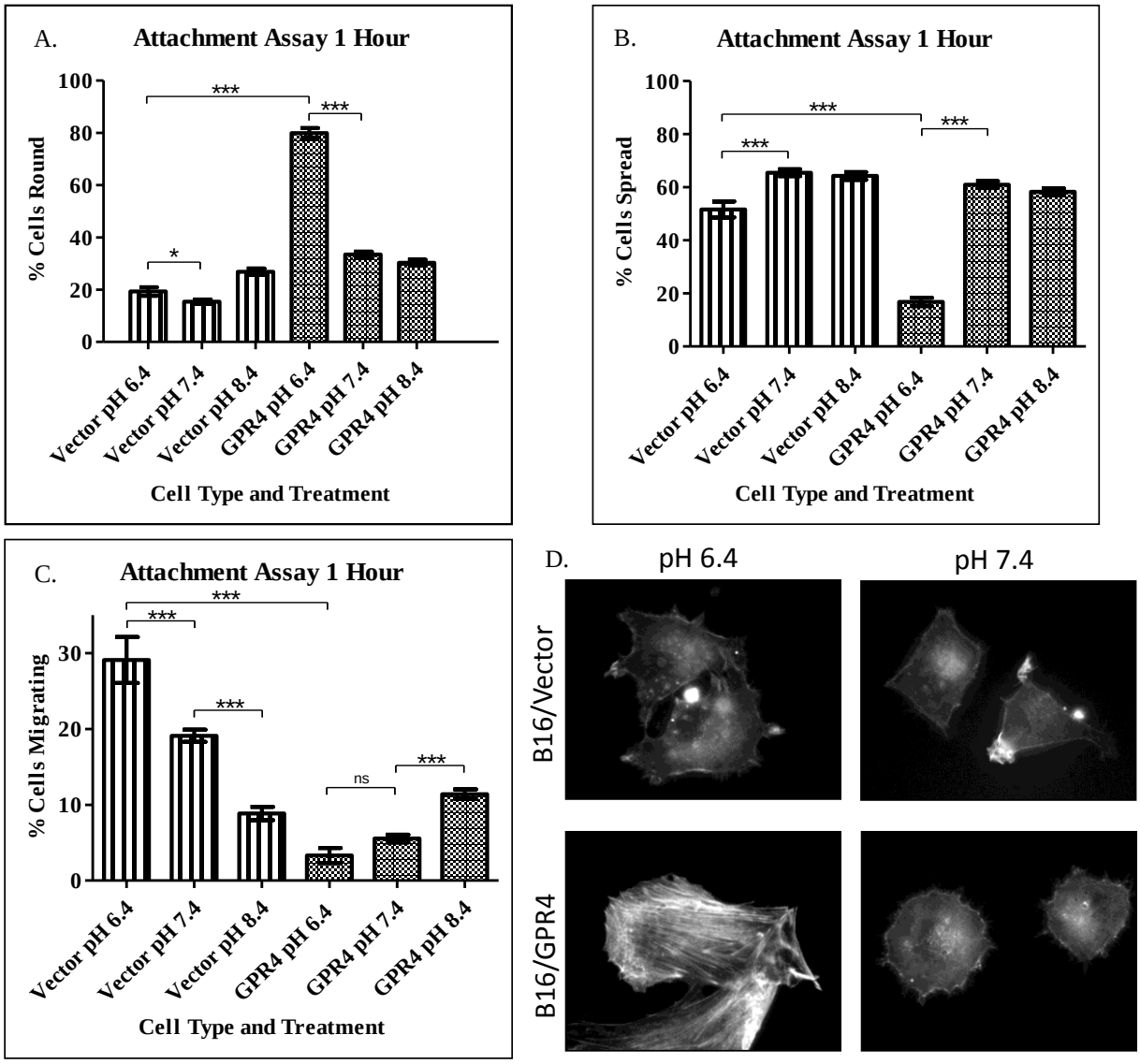

Figure 3. B16/Vector and B16/GPR4 Cell Spreading and Actin Stress Fiber Development. (A) Percent of round B16/Vector and B16/GPR4 cells after a one-hour attachment assay at pH 6.4, 7.4, or 8.4. (B) Percent of spread B16/Vector and B16/GPR4 cells after a one-hour attachment assay at pH 6.4, 7.4, or 8.4. (C) Percent of migrating B16/Vector and B16/GPR4 cells after a one-hour attachment assay at pH 6.4, 7.4, or 8.4. (D) B16/Vector and B16/GPR4 cell actin staining after a one hour treatment with DMEM w/o FBS buffered to pH 6.4 or 7.4. For quantification 10-40 fields of view (FOV) in each treatment group in A, B, and C was analyzed (1-4 wells). There was roughly 30-40 cells/FOV. (*** $P < .001$, * $P < .05$, ns $P > .05$)

B16/GPR4 Cell Spreading is Delayed on Various Substrates

B16F10 melanoma cell spreading was also examined on several substrates such as glass coverslips, fibronectin coated glass coverslips, and matrigel. Following a one-hour attachment assay the B16/GPR4 cells displayed delayed spreading on all three substrates when compared to B16/Vector cells at pH 6.4 (Figure 4A-F). When compared to B16/Vector cells, the majority of B16/GPR4 cells were round one hour after plating (Figure 4B, D, and F). Both cell lines displayed cell spreading similar to when plated on tissue culture plates at pH 6.4 (Figure 2A-B compared to Figure 4A-F).

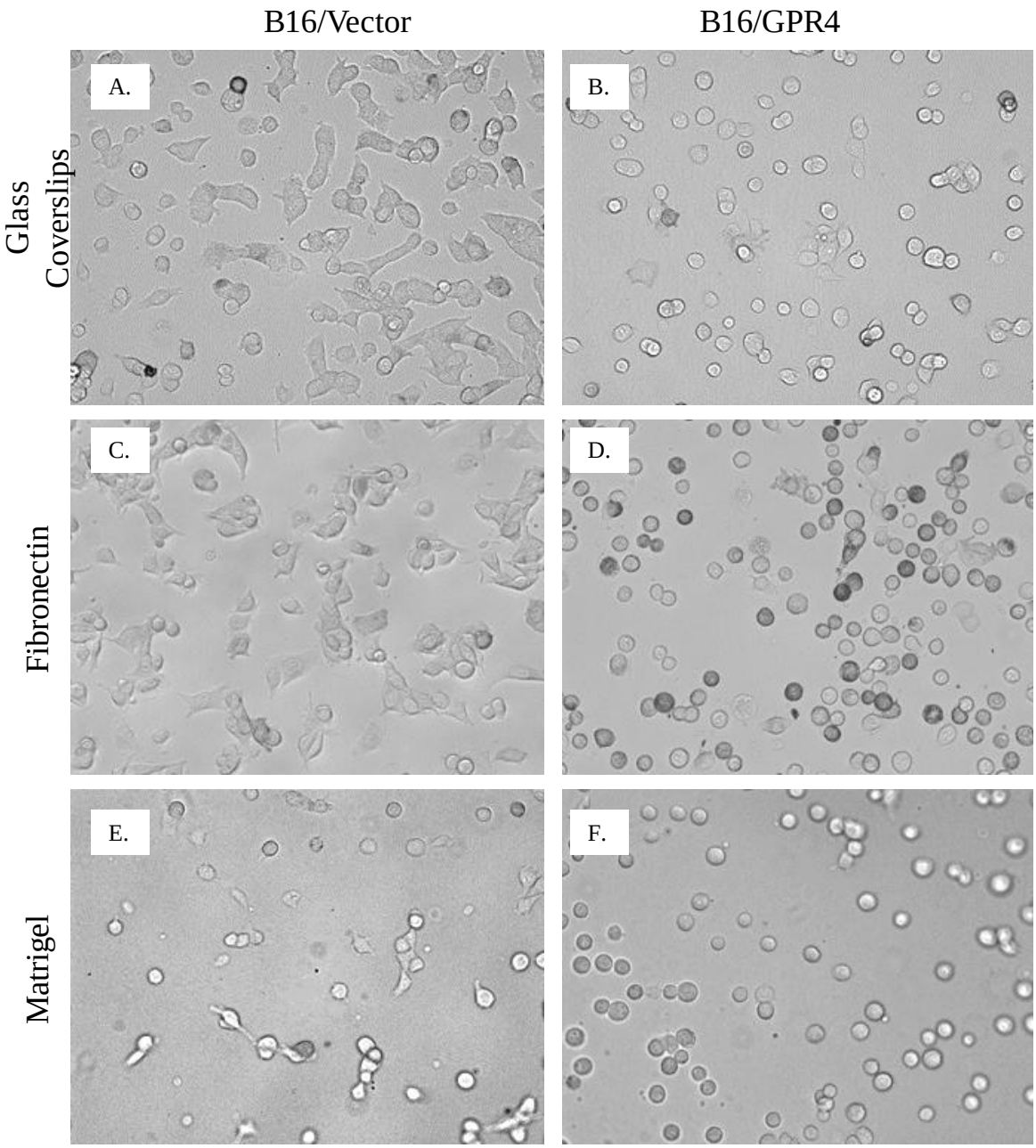

Figure 4. B16/Vector and B16/GPR4 Cell Spreading on Various Substrates at pH 6.4. (A) and (B) B16/Vector and B16/GPR4 cell glass coverslip one-hour attachment assay. (C) and (D) B16/Vector and B16/GPR4 cell fibronectin coated glass coverslip one-hour attachment assay. (E) and (F) B16/Vector and B16/GPR4 cell matrigel one-hour attachment assay.

GPR4 Activation Significantly Delays B16/GPR4 Cell Spreading on Matrigel

In previous in vivo studies, lung metastasis was reduced following tail vein injections in mice due to the overexpression of GPR4 in B16F10 cells (15). To investigate B16F10 cell attachment and spreading on alternate substrates we decided to use matrigel due to its similarity to lung tissue. To begin, matrigel was thawed on ice for one hour and enough matrigel was plated to generate a thick gel in the wells of a 96-well plate. After the matrigel solidified into a gel, B16F10 melanoma cells were plated on it in DMEM supplemented with 10% FBS buffered to pH 6.4, 7.4, or 8.4. One hour later, 5 pictures were taken of each well at 200X total magnification and the round, spread, and migrating cell percentages were calculated using the same quantification method used in the tissue culture plate attachment assays (Figure 3A-C). The B16/GPR4 cells behaved very much the same way and differed only slightly in round, spread, or migrating cell percentages. When compared to tissue culture plate attachment and spreading percentages, there was a small increase in the B16/GPR4 round cell percentage at pH 6.4 from 80% to 85% and the migrating cell percentage was reduced from 3.3% to .8% (Figure 3A and 5A). The B16/Vector cells, however, displayed a decrease in the round cell percentage from 19% to 14%, but also displayed a decrease in their migrating cell percentage from 29% to 18%, respectively (Figure 4A and 5A). Overall, the spreading of B16/GPR4 cells was substantially inhibited at pH 6.4 in comparison to B16/Vector cells (Figure 5A-C). Furthermore, the B16/Vector cells again displayed an increased percentage of migrating cells (Figure 5C). The similarity between the behavior of B16/GPR4 cells on matrigel, fibronectin, glass coverslips, and tissue culture plates signifies a substrate-independent mechanism in which cell spreading is delayed due to the activation of GPR4.

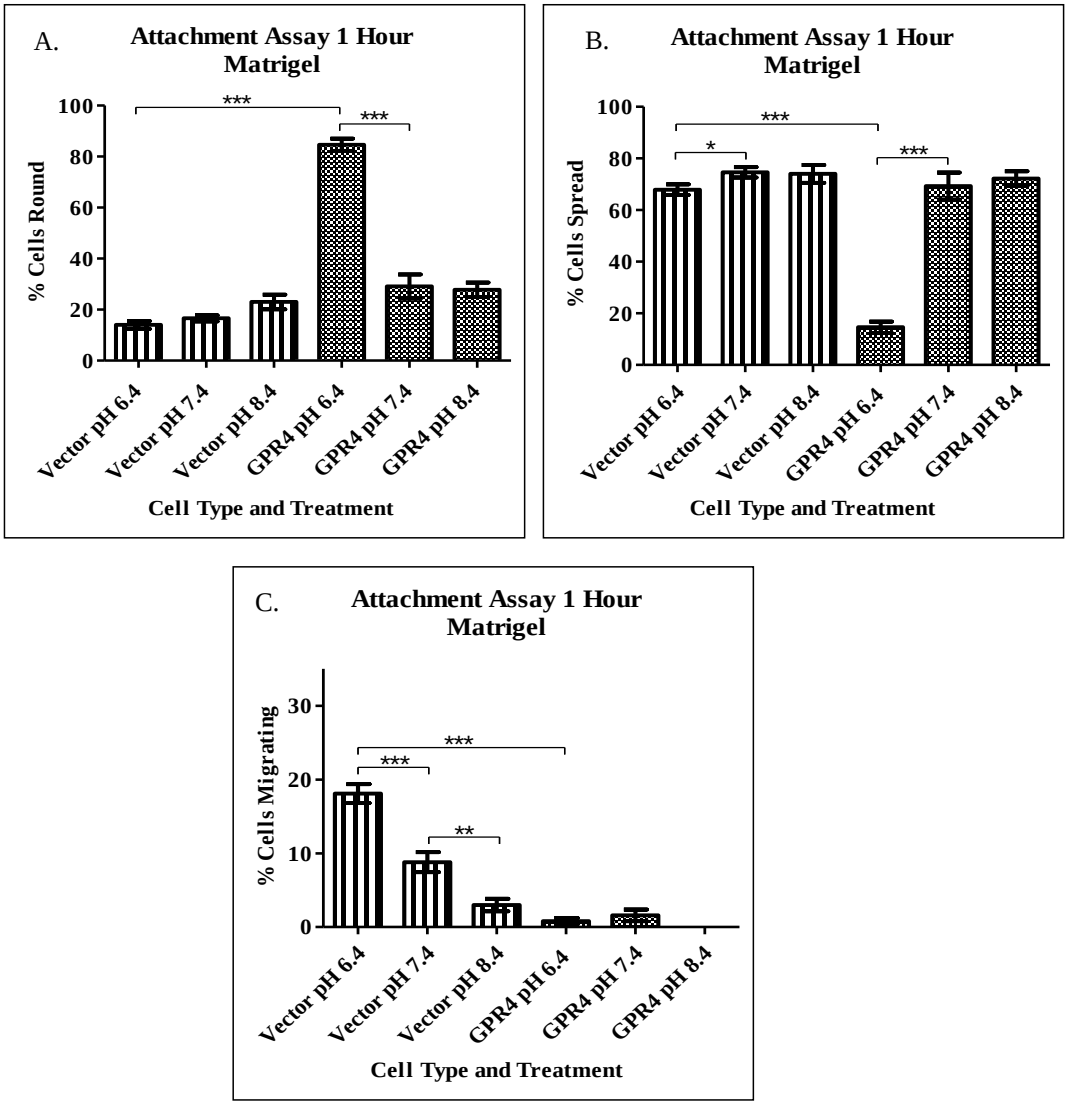

Figure 5. B16/Vector and B16/GPR4 Cell Matrigel Attachment Assay. (A) Percent of round B16/Vector and B16/GPR4 cells after a one-hour attachment assay on matrigel at pH 6.4, 7.4, or 8.4. (B) Percent of spread B16/Vector and B16/GPR4 cells after a one-hour attachment assay on matrigel at pH 6.4, 7.4, or 8.4. (C) Percent of migrating B16/Vector and B16/GPR4 cells after a one-hour attachment assay on matrigel at pH 6.4, 7.4, or 8.4. For quantification 10 fields of view (FOV) in each treatment group in A, B, and C was analyzed (2 wells). There was roughly 30-40 cells/FOV. (*** $P < .001$, ** $P < .01$, * $P < .05$)

Treatment with Either C3-Transferase (CT04) or an Inhibitory $G_{12/13}$ Construct Significantly Restores B16/GPR4 Cell Spreading and Reduces Actin Stress Fiber Development

To delineate the specific intracellular signaling pathway that is activated in B16/GPR4 cells when GPR4 is active we first used C3-transferase (CT04). CT04 is a cell permeable Rho inhibitor that reduces its activation significantly by ADP-ribosylation on Asparagine 41 of the effector-binding domain of Rho-GTPase. B16/GPR4 cells were treated with .75 µg/mL and 2.0 µg/mL CT04 at the time of plating and throughout the duration of the one-hour attachment assays. The percentage of round cells was 51% and 36%, respectively. Both of the concentrations used restored B16/GPR4 cell spreading significantly. All subsequent experiments were completed with 2.0 µg/mL CT04 (Figure 6A). The restoration in cell spreading following treatment with a Rho inhibitor signifies its involvement in B16/GPR4 cell's delayed cell spreading at pH 6.4.

To further demonstrate that Rho activation may be the reason for delayed B16/GPR4 cell spreading at pH 6.4 we attempted to recapitulate their phenotype in the B16/Vector cells. In order to reveal the role that Rho activation plays during B16F10 melanoma cell spreading we used a commonly used indirect Rho activator, CN01, or otherwise known as Calpeptin. Calpeptin acts to indirectly stimulate the activation of Rho by inhibiting SH2 phosphatase, which normally deactivates Rho-Guanine nucleotide Exchange Factors (GEFs). Therefore, B16/Vector cells should potentially demonstrate a reduction in cell spreading that is comparable to B16/GPR4 cells at pH 6.4 if Rho activation is responsible for delayed B16/GPR4 cell spreading. B16/Vector cells were treated with .25 Unit/mL, .5 Unit/mL, and 1.0 Unit/mL CN01 at the time of plating and throughout the duration of the one-hour attachment assays. The percentage of

round cells was 42%, 67%, and 77%, respectively. All of the CN01 concentrations used inhibited B16/Vector cell spreading significantly but only 1.0 Unit/mL CN01 treatment is graphed in figure 6A.

Having proven that Rho activation may delay B16/GPR4 cell spreading by using chemical activators and inhibitors, it was decided to further connect activation of GPR4 to the $G_{12/13}$ G-protein signaling pathway. To do this, a $G_{12/13}$ inhibitory construct was transduced into the B16/GPR4 cells (95). By using this inhibitory construct in B16/GPR4 cells the interaction of the $G_{12/13}$ G-protein and P115 Rho-GEF should be inhibited (39). After completing attachment assays at pH 6.4 we determined that when treated with media buffered to pH 6.4, B16/GPR4 $G_{12/13}$- cells demonstrated a round cell percentage that was 35% comparable to 36% in B16/GPR4 cells treated with CT04 at pH 6.4 (Figure 7A and 6A). The B16/GPR4 PQCXIP control cell line exhibited the same percentage of round cells as seen in B16/GPR4 cells at pH 6.4 (Figure 7A). The restoration of cell spreading found in the B16/GPR4 $G_{12/13}$- cells and when CT04 is applied to B16/GPR4 cells demonstrate that when GPR4 is activated, it activates the $G_{12/13}$ G-protein and subsequently Rho is activated, which possibly leads to increased cytoskeletal tension and an alteration in cell spreading dynamics.

Previously, B16/GPR4 cell Rho-GTP levels were reported increased at pH 6.4 and stress fibers were markedly present (15). To indirectly examine the activation of Rho and the level of cytoskeletal tension Rhodamine phalloidin was used to stain for actin stress fibers. Following serum starvation and treatment with DMEM buffered to pH 6.4 for one hour actin stress fibers in B16/GPR4 $G_{12/13-}$ cells were absent. This demonstrates a reduction in Rho activation and cytoskeletal tension (Figure 7E). Furthermore, CT04 treatment (2.0 µg/mL) in B16/GPR4 cells at pH 6.4 also reduced actin stress fibers (Figure 6C). This positively demonstrates that there is a

correlation between $G_{12/13}$/Rho activation, cytoskeletal tension, and B16/GPR4 cell spreading at pH 6.4.

In addition, to determine if the restoration in B16/GPR4 cell spreading is occurring on another substrate B16/GPR4 $G_{12/13-}$ and B16/GPR4 PQCXIP cell one-hour attachment assays were performed at pH 6.4, 7.4, and 8.4 on matrigel (Figure 8A). The B16/GPR4$_{12/13}$- cells at pH 6.4 displayed a round cell percentage of 21% versus the 80% round cell percentage found in the B16/GPR4 empty vector control cell line (Figure 8A). The restoration in B16/GPR4 $G_{12/13}$- cell spreading following attachment onto a matrigel surface continues to reveal that the B16/GPR4 cell attachment and spreading alterations may be caused by intracellular Rho activation/cytoskeletal tension and not alternate substrates.

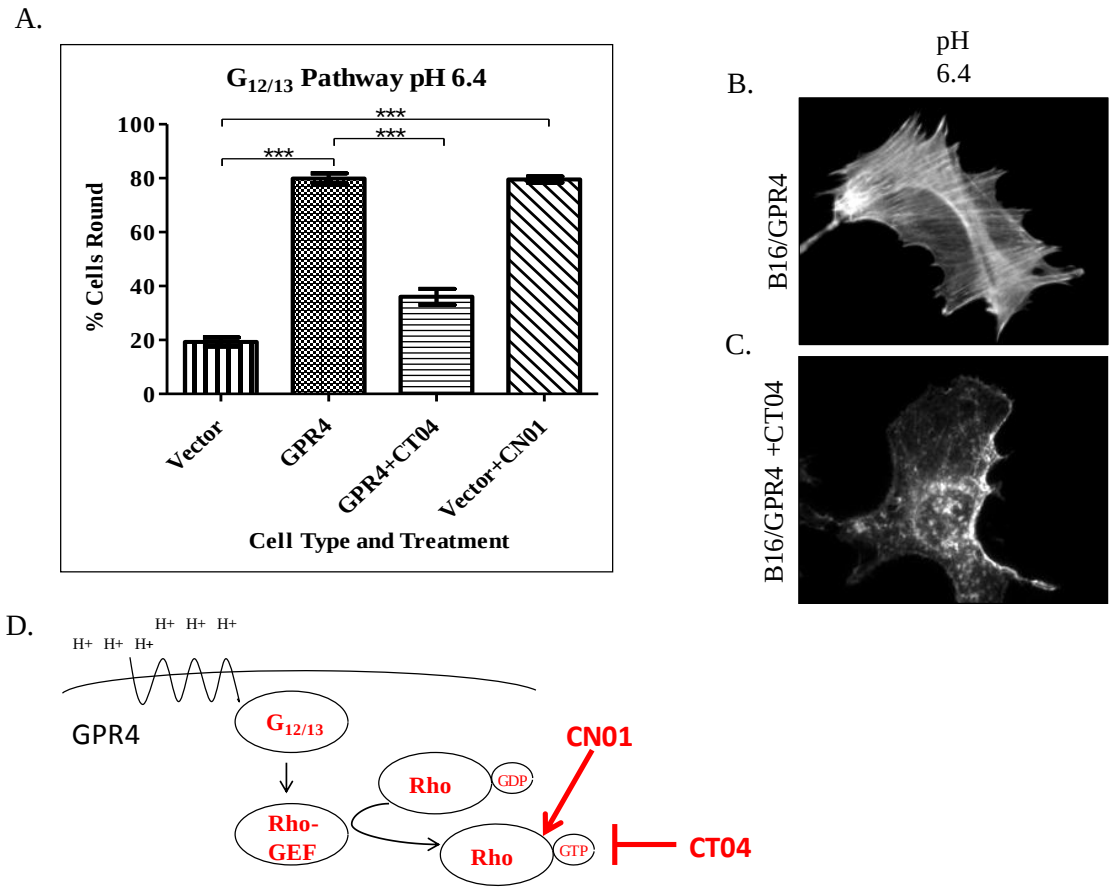

Figure 6. Rho Signaling in B16/Vector and B16/GPR4 Cell Spreading and Stress Fiber Development. (A) $G_{12/13}$ pathway chemical manipulations of B16/Vector and B16/GPR4 cells. (B) and (C) B16/GPR4 cell actin staining following 2 µg/mL CT04 treatment for 1 hour. (D) Diagram depicting chemical activator and inhibitor effects on the $G_{12/13}$ signaling pathway. For quantification 10-40 fields of view (FOV) in each treatment group in A was analyzed (1-4 wells). There was roughly 30-40 cells/FOV. (*** P < .001)

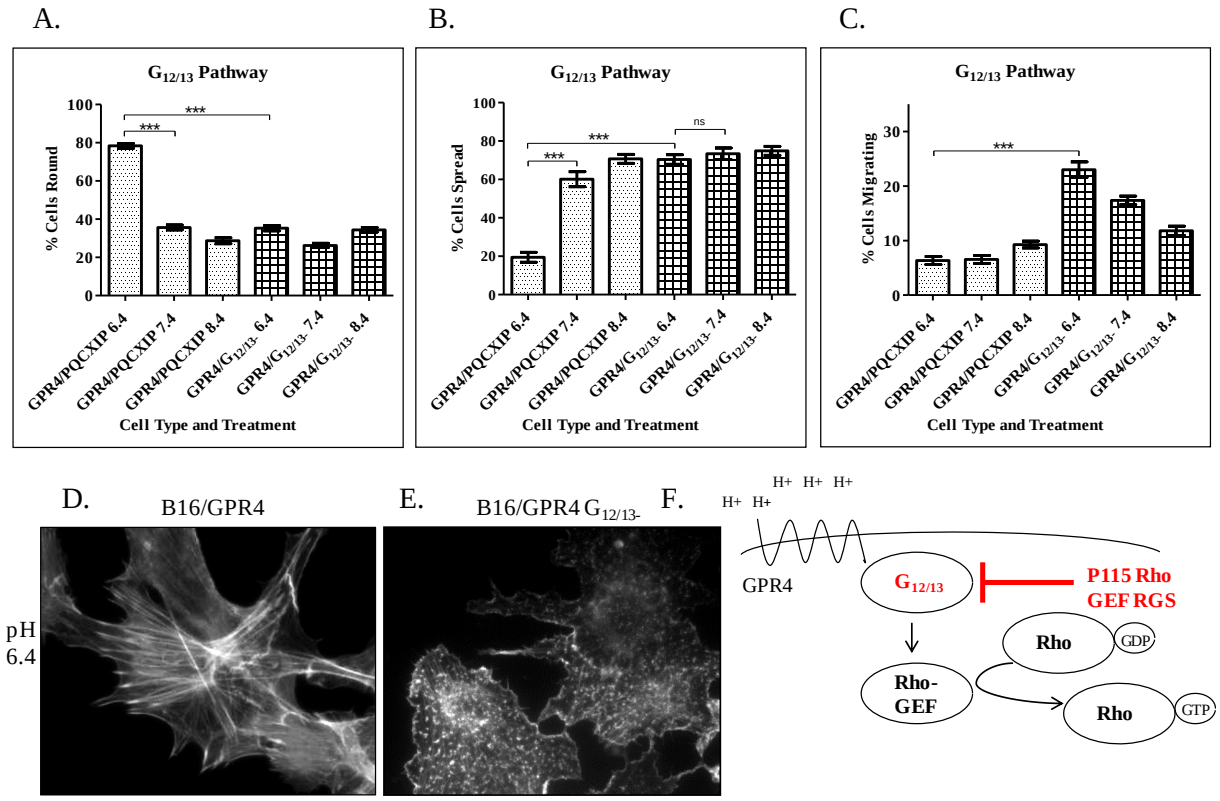

Figure 7. $G_{12/13}$ Signaling in B16/GPR4 Cell Spreading and Actin Stress Fiber Development. (A) Percent of round B16/GPR4 PQCXIP and B16/GPR4 $G_{12/13-}$ cells after a one-hour attachment assay at pH 6.4, 7.4, or 8.4. (B) Percent of spread B16/GPR4 PQCXIP and B16/GPR4 $G_{12/13-}$ cells after a one-hour attachment assay at pH 6.4, 7.4, or 8.4. (C) Percent of migrating B16/GPR4 PQCXIP and B16/GPR4 $G_{12/13-}$ cells after a one-hour attachment assay at pH 6.4, 7.4, or 8.4. (D) and (E) B16/GPR4 and B16/GPR4 $G_{12/13-}$ cell actin staining following 1 hour treatment with DMEM buffered to pH 6.4 and 7.4. (F) Diagram depicting the mechanism of action of the P115 Rho GEF RGS inhibitory construct in the $G_{12/13}$ signaling pathway. For quantification 10-40 fields of view (FOV) in each treatment group in A, B, and C was analyzed (1-4 Wells). There was roughly 30-40 cells/FOV. (*** $P < .001$ and ns $P > .05$)

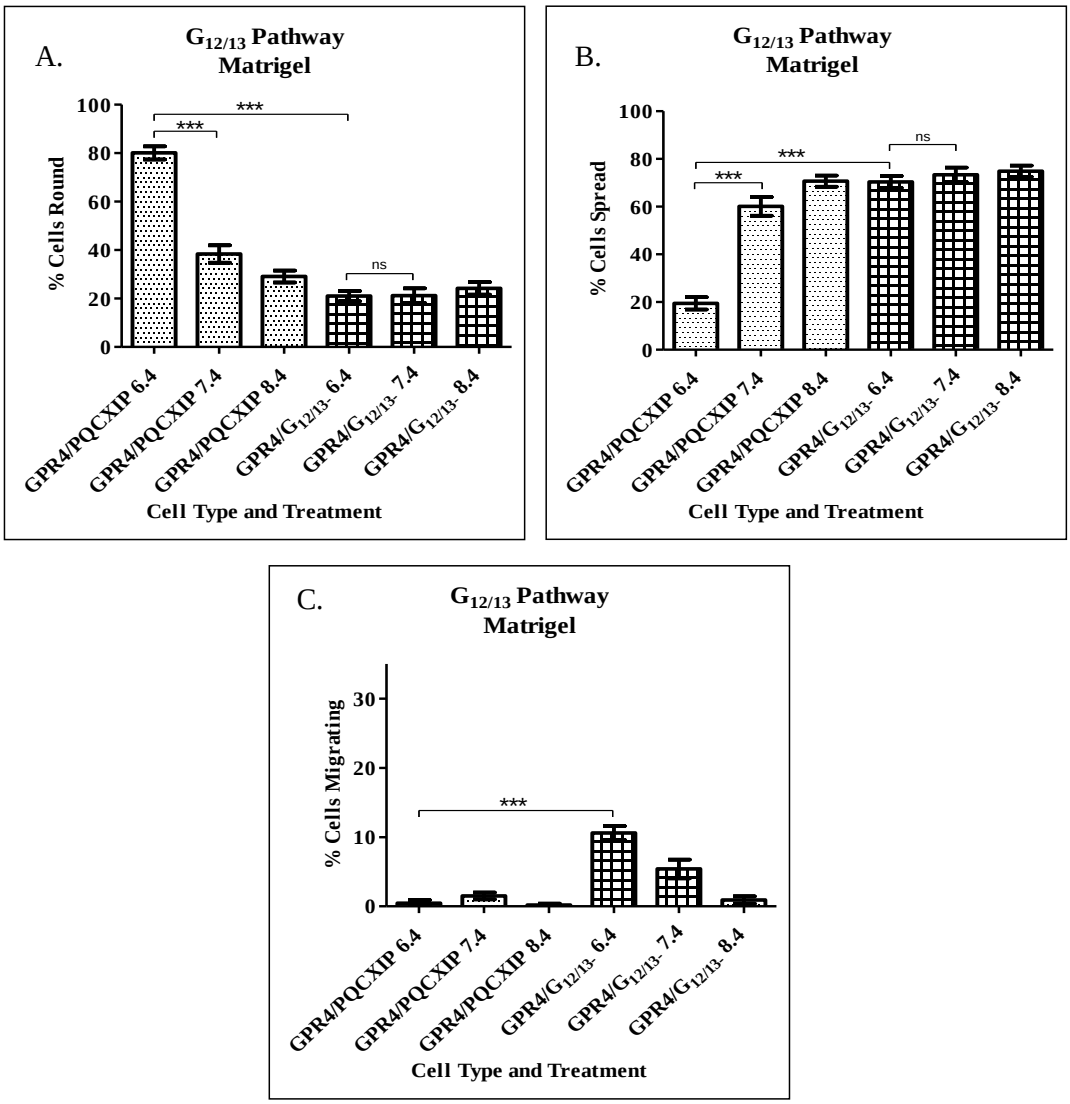

Figure 8. $G_{12/13}$ Signaling in B16/GPR4 Cell Spreading on Matrigel. (A) Percent of round B16/GPR4 PQCXIP and B16/GPR4 $G_{12/13-}$ cells after a one-hour attachment assay at pH 6.4, 7.4, or 8.4. (B) Percent of spread B16/GPR4 PQCXIP and B16/GPR4 $G_{12/13-}$ cells after a one-hour attachment assay at pH 6.4, 7.4, or 8.4. (C) Percent of migrating B16/GPR4 PQCXIP and B16/GPR4 $G_{12/13-}$ cells after a one-hour attachment assay on matrigel at pH 6.4, 7.4, or 8.4. For quantification 10 fields of view (FOV) in each treatment group in A, B, and C was analyzed (2 Wells). There was roughly 30-40 cells/FOV. (*** $P < .001$ and ns $P > .05$)

Y27632 and Staurosporine Restores B16/GPR4 Cell Spreading and Reduces Actin Stress Fiber Development

To further investigate downstream signaling pathways that are active following GPR4 activation at pH 6.4, the Rho kinase (ROCK) inhibitor Y27632 was used during a one-hour B16/GPR4 cell attachment assay at pH 6.4. B16/GPR4 cells were treated with 1 µM, 10 µM, and 50 µM Y27632 at pH 6.4 at the time of plating and for the duration of the one-hour attachment assays. The percentage of round cells was 67%, 60%, and 59%, respectively. Subsequent experiments were performed with 10 µM Y27632 (Figure 9A). Successive statistical analysis revealed that B16/GPR4 cell spreading was significantly restored (Figure 9A). Next, the kinase inhibitor Staurosporine (STA) was used during a one-hour attachment assay. B16/GPR4 cells were treated with 1.3 nM, 2.0 nM, and 4.0 nM STA at pH 6.4 at the time of plating and for the duration of the one-hour attachment assays. At 1.3 nM the STA product data sheet states that MLCK is inhibited. The percentage of round cells was 26%, 31%, and 30%, respectively. Subsequent experiments were performed with 1.3 nM STA (Figure 9B). Successive statistical analysis revealed that B16/GPR4 cell spreading was restored in all treatment groups (Figure 9B). This signifies that Rho may activate Rho kinase and subsequently increase MLC phosphorylation to increase cytoskeletal tension and delay the initial stages of B16/GPR4 cell spreading at pH 6.4.

In addition, Y27632 (10µM) was used to inhibit ROCK activity in B16/GPR4 cells at pH 6.4 for one hour before actin staining. A decrease in ROCK activity may reduce MLC phosphorylation by inhibiting its function of phosphorylating and deactivating MLC phosphatase (Figure 9F) (25 and 26). Also ROCK inactivation may reduce MLC phosphorylation by interrupting the potential for direct phosphorylation of MLC at serine 19 by ROCK (Figure 9F)

(81). The results displayed a reduction in actin stress fiber development following treatment with Y27632 (Figure 9D). This further correlates with an increase in B16/GPR4 cell spreading at pH 6.4 when treated with Y27632 during a one-hour attachment assay (Figure 9A). Lastly, Staurosporine (1.3nM) was used to inhibit MLCK activity for one hour at pH 6.4 before actin staining, which may potentially decrease the phosphorylation of MLC and eventually lead to reduced cytoskeletal tension and stress fiber development (Figure 9F). The results were concordant with the hypothesis and actin stress fibers were absent following treatment with acidic media and Staurosporine for one hour in B16/GPR4 cells (Figure 9E). These results are correlative with restored B16/GPR4 cell spreading following one-hour attachment assays to tissue culture plates and Staurosporine treatment at pH 6.4 (Figure 9B).

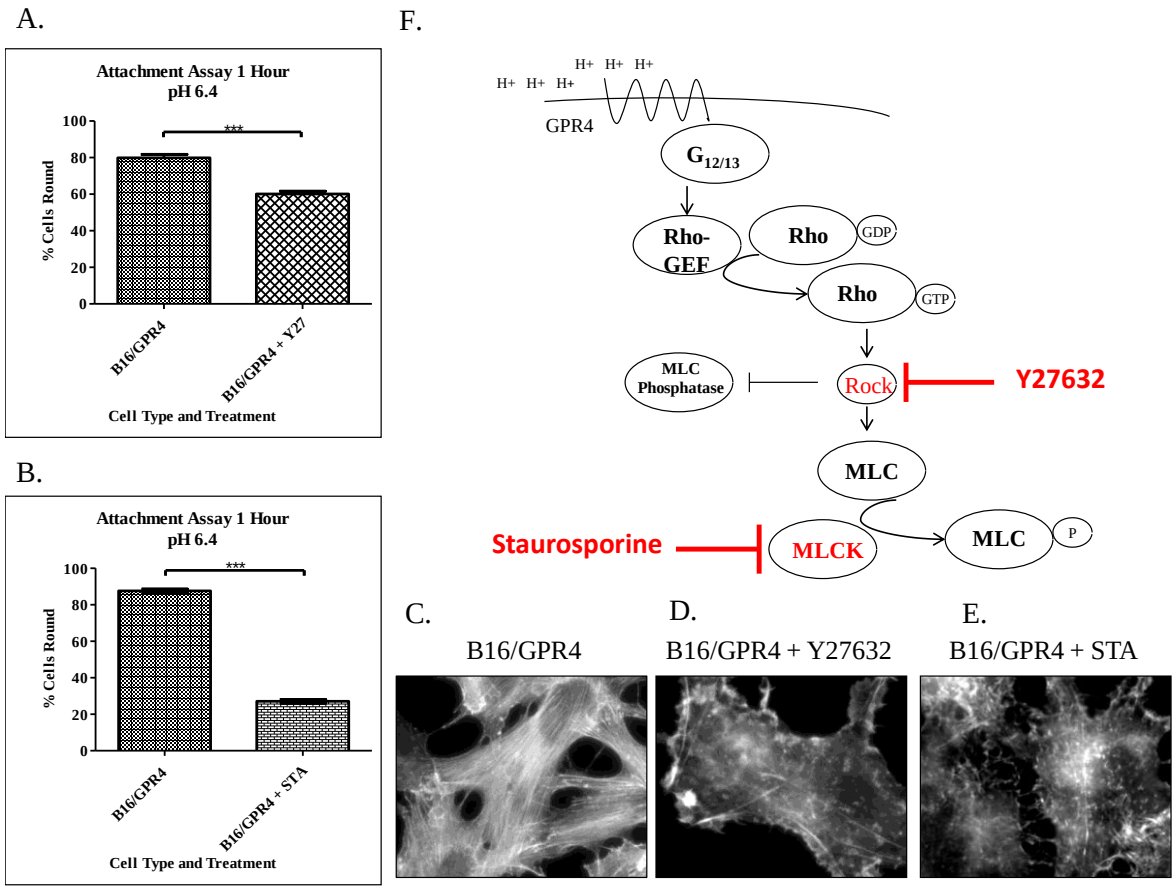

Figure 9. Downstream $G_{12/13}$ Signaling Pathways in B16/GPR4 Cell Spreading and Actin Stress Fiber Development. (A) Percent of round B16/GPR4 cells after a one-hour attachment assay at pH 6.4 and ROCK chemical manipulations. (B) Percent of round B16/GPR4 cells after a one-hour attachment assay at pH 6.4 and MLCK chemical manipulations. (C) (D) and (E) Actin staining of B16/GPR4 cells following a one hour treatment with DMEM buffered to pH 6.4 and 10µM Y27632 or 1.3nM Staurosporine.(F) Diagram depicting the action of the kinase inhibitors used. For quantification 10-40 fields of view (FOV) in each treatment group in A and B was analyzed (1-4 Wells). There was roughly 30-40 cells/FOV. (*** P < .001)

The Activation/Inhibition of the G_q and G_s G-protein Signaling Pathways Does Not Affect B16F10 Cell Spreading on Tissue Culture Plates or Matrigel

To investigate other G-protein pathways that may be activated in B16/GPR4 cells when treated with acidic media that may potentially contribute to delayed cell spreading the G_q and G_s pathways were examined. To initiate our inquiry we began by simulating the activation of the G_s G-protein pathway in B16/Vector cells. First, 8-bromo-cAMP, a cell permeable cAMP analogue that is resistant to degradation was utilized. The cAMP analogue, 8-bromo-cAMP increases cytosolic cAMP levels and therefore the signaling pathways that are activated when the G_s pathway is stimulated are also activated (Figure 10C). Cells were treated with 8-bromo-cAMP at 100 µM, 500 µM, and 750 µM concentrations at the time of plating and throughout the duration of the one-hour attachment assays. The percentage of round cells was 28%, 28%, and 31% compared to 29% round cells in the control B16/Vector sample. Successive experiments were carried out with 500µM 8-bromo-cAMP. Following one-hour attachment assays with 8-bromo cAMP (500µM) at pH 6.4, the round B16/Vector cell percentage changed from 19% to 17%, which was not statistically significant (Figure 10A).

Next, 2', 5'-dideoxyadenosine (DDA), an adenylyl cyclase inhibitor, was used to inhibit adenylyl cylcase activity in B16/GPR4 cells at pH 6.4 (Figure 10C). A decrease in adenylyl cyclase activity should inhibit the signaling pathway that is used to increase cytosolic cAMP levels (Figure 10C). Therefore, if G_s/cAMP stimulation is involved in the delay of B16/GPR4 cell spreading at pH 6.4, it should allow for efficient cell spreading. Cells were treated with DDA at 10 µM, 100 µM, and 200 µM concentrations at the time of plating and for the duration of the one-hour attachment assays. The percentage of round cells was 86%, 85%, and 88% compared to 84% in the control B16/GPR4 cell sample. Successive experiments were carried out with 100µM

DDA (Figure 10A). The round cell percentage did not vary significantly from the B16/GPR4 cell control (Figure 10A). Following G_s G-protein alterations in several B16F10 melanoma cell lines, it was determined that the G_s signaling pathway is not responsible for the cell spreading defect found in B16/GPR4 cells when stimulated with acidic media.

The G_q signaling pathway has been previously reported active following activation of GPR4 (79). To examine whether the G_q pathway is involved in delayed B16/GPR4 cell spreading, the activation of the G_q pathway in B16/Vector cells was simulated. Following G_q activation and the stimulation of several signaling pathways, calcium is released from the endoplasmic reticulum into the cytosol of the cell and from there it affects the activity of several proteins (Table 1) (1). To simulate G_q pathway activation, thapsigargin, a chemical known to increase intracellular calcium levels was used (Figure 10C). To investigate the possibility of G_q involvement in B16/GPR4 cell spreading, tissue culture plate cell attachment assays were utilized. B16/Vector cells were treated with 10 nM, 100 nM, and 500 nM thapsigargin at the time of plating and throughout the duration of the one-hour attachment assays. The percentage of round cells was 29%, 25%, and 27% compared to 26% in the control B16/Vector cell sample. Successive experiments were carried out with 500 nM thapsigargin (Figure 10B). Treatments with thapsigargin (500nM) during one-hour attachment assays at pH 6.4 established that there was no significant effect on B16/Vector cell spreading (Figure 10B).

To further examine the role that the G_q protein may have in B16/GPR4 cells during cell spreading, a G_q signaling inhibitory construct was transduced into the B16/GPR4 cells. The G_q inhibitory construct should reduce G_q G-protein signaling through GRK2 RGS and if it is involved in B16/GPR4 cell spreading at pH 6.4 then cell spreading should be restored (Figure 11D) (13). There was not a significant alteration in cell spreading at pH 6.4 in B16/GPR4 G_q-

cells on tissue culture plates or matrigel and they closely resembled the B16/GPR4 and B16/GPR4 PQCXIP cells with a round cell percentage of 79% (Figure 11A and 12A). Following these chemical treatments and the use of a G_q inhibitory construct, it has been determined that the G_q G-protein pathway is not responsible for the delayed cell spreading found in B16/GPR4 cells at pH 6.4.

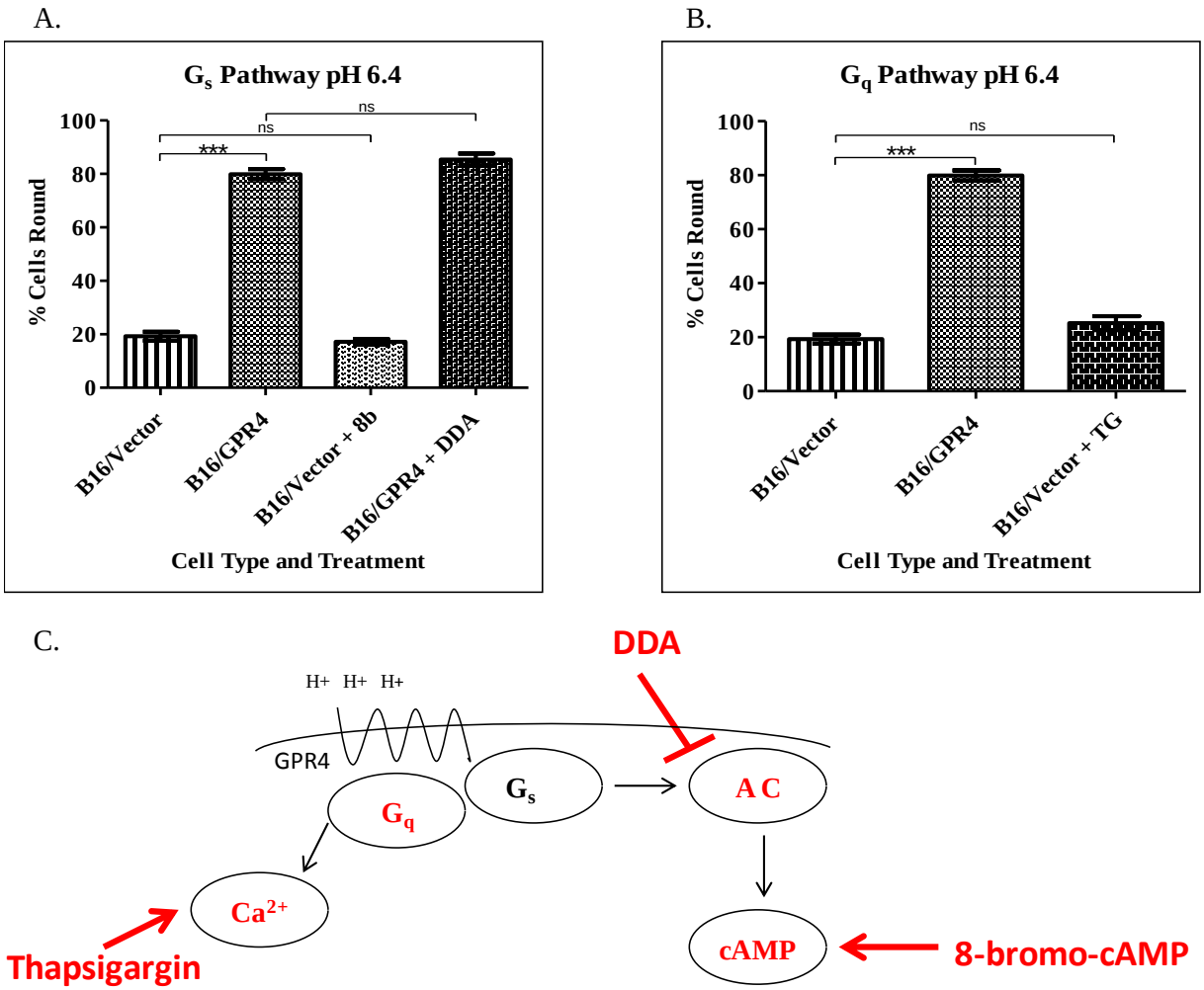

Figure 10. Downstream G_s and G_q Signaling in B16/Vector and B16/GPR4 Cell Spreading. (A) Percent of round B16/Vector and B16/GPR4 cells after a one-hour attachment assay at pH 6.4 and G_s pathway chemical manipulations. (B) Percent of round B16/Vector and B16/GPR4 cells after a one-hour attachment assay at pH 6.4 and G_q pathway chemical manipulations.(C) Diagram depicting the action of drugs 500µM 8-bromo-cAMP (8b), 100µM DDA, or 500nM thapsigargin (TG) on the G_s or G_q signaling pathways. For quantification 10-40 fields of view (FOV) in each treatment group in A and B was analyzed (1-4 Wells). There was roughly 30-40 cells/FOV. (*** $P < .001$ and ns $P > .05$)

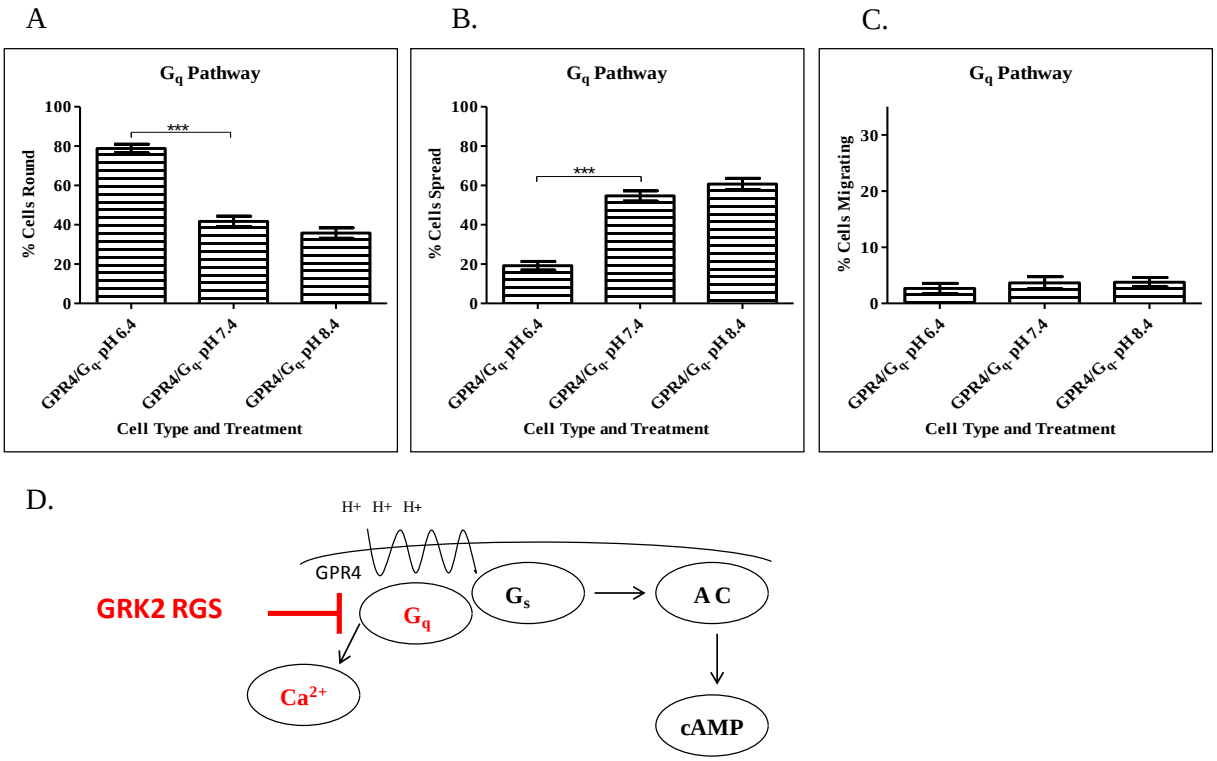

Figure 11. G_q Signaling in B16/GPR4 Cell Spreading. (A) Percent of round B16/GPR4 G_{q-} cells after a one-hour attachment assay at pH 6.4, 7.4, or 8.4. (B) Percent of spread B16/GPR4 G_{q-} cells after a one-hour attachment assay at pH 6.4, 7.4, or 8.4. (C) Percent of migrating B16/GPR4 G_{q-} cells after a one-hour attachment assay at pH 6.4, 7.4, or 8.4. (D) Diagram depicting the mechanism of action of the GRK2 RGS inhibitory construct in the G_q signaling pathway. For quantification 10-40 fields of view (FOV) in each treatment group in A, B, and C was analyzed (1-4 Wells). There was roughly 30-40 cells/FOV. (*** $P < .001$)

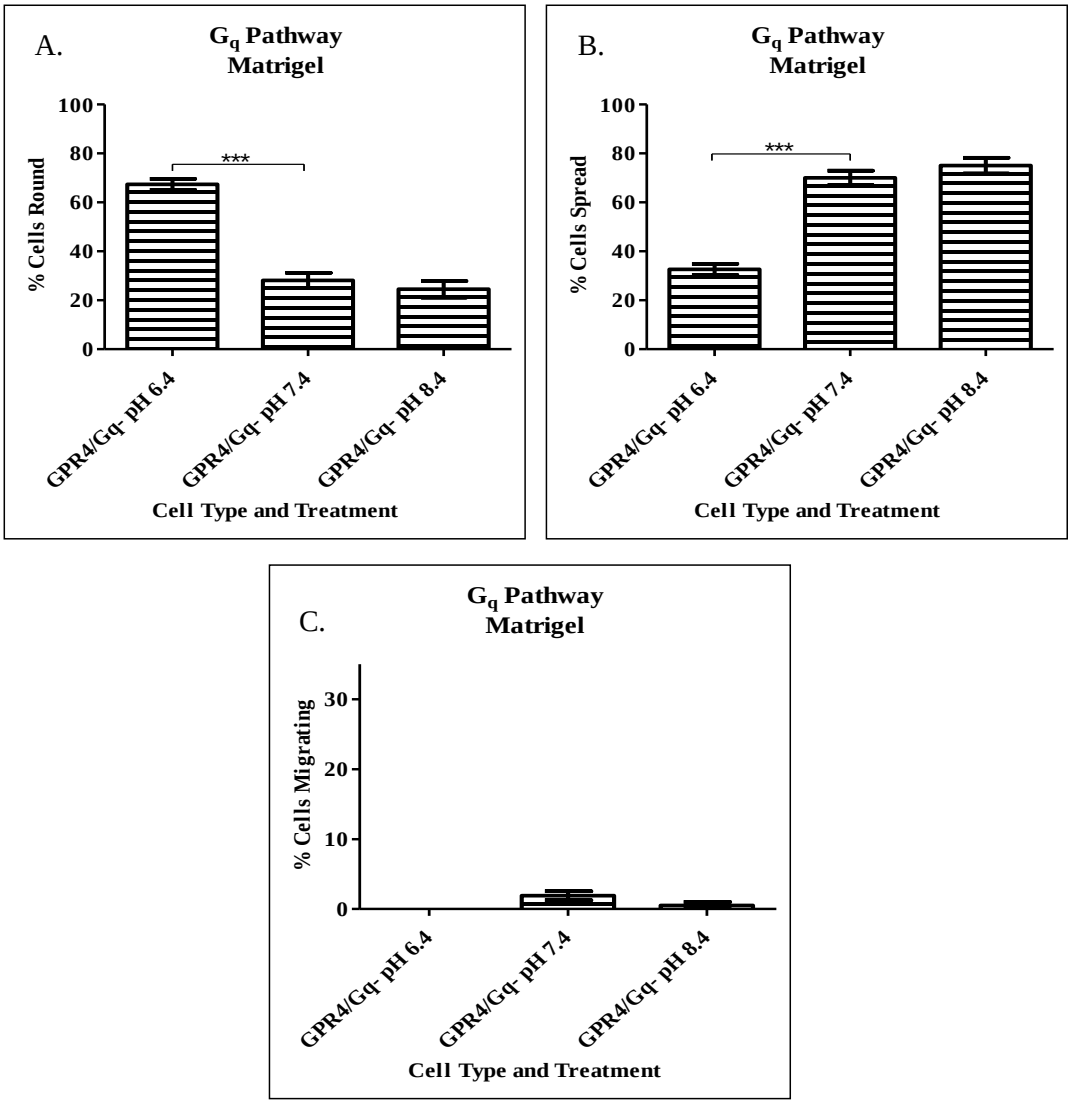

Figure 12. G_q Signaling in B16/GPR4 Cell Spreading on Matrigel (A) Percent of round B16/GPR4 G_{q-} cells after a one-hour attachment assay on matrigel at pH 6.4, 7.4, or 8.4. (B) Percent of spread B16/GPR4 G_{q-} cells after a one-hour attachment assay on matrigel at pH 6.4, 7.4, or 8.4. (C) Percent of migrating B16/GPR4 G_{q-} cells after a one-hour attachment assay on matrigel at pH 6.4, 7.4, or 8.4. For quantification, 10 fields of view (FOV) in each treatment group in A, B, and C was analyzed (2 Wells). There was roughly 30-40 cells/FOV. (*** $P < .001$)

Activation of GPR4 Alters the Localization of Phospho-Paxillin (Y118) in B16/GPR4 Cells during Attachment and Spreading

Focal adhesion dynamics are extremely important for cell spreading as well as migration. For efficient cell attachment, spreading, and movement, focal adhesions must undergo focal adhesion formation and shortly after they must be broken down in order for focal adhesion turnover to occur. To investigate a possible alteration in focal adhesion dynamics during B16/GPR4 cell spreading we inspected the phospho-protein phospho-paxillin (Y118). Several sources confirm that phospho-paxillin (Y118) is the first focal adhesion protein to localize to dynamic focal adhesions and its localization may determine where newly formed or deteriorating focal adhesions are situated (97). The localization of phospho-paxillin (Y118) at pH 6.4 in B16/GPR4 cells following one-hour attachment assays were localized to the cell body and absent from the cell periphery where membrane ruffling occurs (Figure 13A and 13B). Total paxillin, however, was localized to the cell periphery and displayed the same results in every cell line in each treatment group (Figure 13D). To quantify the percentage of B16/GPR4 cells displaying the altered phenotype after a one-hour attachment, the percentage of cells with peripheral localization versus cell body localization was determined by taking photos of attached cells at 1000X total magnification of several samples. Out of 100 or more cells, single cells were determined to either have peripheral localization or cell body localization (Figure 13C). The percentage of cells with phospho-paxillin (Y118) localized to the cell body in B16/GPR4 cells after a one-hour attachment at pH 6.4 was 93.2% and 6.8% was localized to the cell periphery (Figure 13C). When treated with pH 7.4-buffered media, phospho-paxillin (Y118) is relocated from the cell body back to the cell periphery, which is similar to what is seen in the B16/Vector cells in all treatment groups (Figure 13A and 13C). The percentage of B16/GPR4 cells with

phospho-paxillin (Y118) localization to the cell body at pH 7.4 was 9.7% and to the cell periphery 90.3% (Figure 13C). In B16/Vector cells, due to highly efficient membrane ruffling and dynamic cell movement viewed by time-lapse photography (98), phospho-paxillin (Y118) signal is localized to the cell periphery at pH 6.4, 7.4, and 8.4 (Figure 13A, B, and C). Moreover, B16/Vector cells lacked significant phospho-paxillin (Y118) signal in the cell body, differing from the B16/GPR4 cells when treated with acidic media (Figure 13A). The percentage of B16/Vector cells displaying a phenotype similar to that of B16/GPR4 cells at pH 6.4 were slim with cell body localization percentages ranging from 7-9% in B16/Vector cells at pH 6.4 and pH 7.4 (Figure 13C). The peripheral localization percentages were high ranging from 91-93% in the B16/Vector cells at pH 6.4 and pH 7.4, opposite of the B16/GPR4 cells at pH 6.4 (Figure 13C).

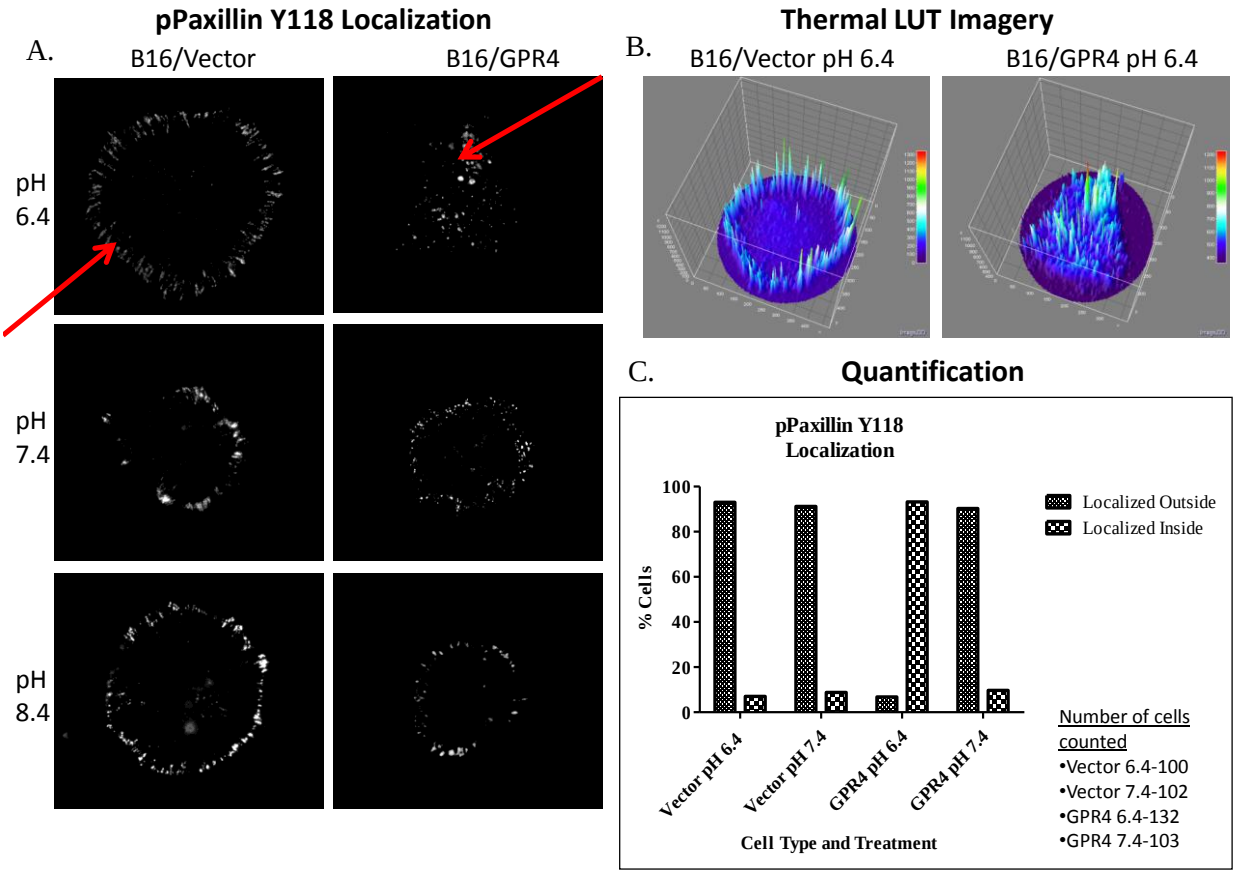

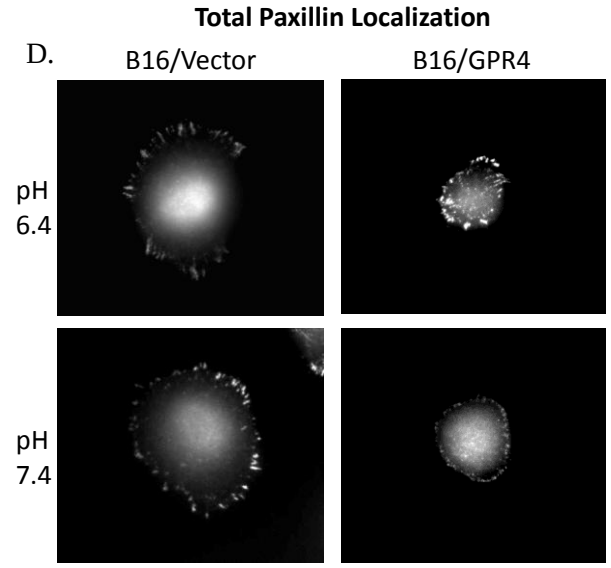

Figure 13. B16/Vector and B16/GPR4 Cell Phospho-Paxillin (Y118) and Total Paxillin Immunocytochemistry. (A) Localization of phospho-paxillin Y118 in B16/Vector and B16/GPR4 cells. (B) A surface plot of the emission signal using Thermal LUT, which represents the localization of phospho-paxillin Y118 in B16/Vector and B16/GPR4 cells. (C) Quantification of cell body (inside) or peripheral localization (outside) of phospho-paxillin Y118. (D) Total paxillin localization in B16/Vector and B16/GPR4 Cells. Repeated 3 times. Please note that B16/GPR4 cells have a smaller circumference due to delayed cell spreading in A and D.

Activation of GPR4 Alters the Localization of Phospho-Focal Adhesion Kinase (FAK) (Y397) in B16/GPR4 Cells during Attachment and Spreading

To further investigate cell spreading during B16/GPR4 cell attachment, phospho-FAK (Y397) localization was explored. Focal adhesion kinase is an extremely important focal adhesion protein responsible for several cell processes (53). It is activated by integrin clustering as well as interaction of the SH2 domain of SRC kinase with focal adhesion kinase's autophosphorylation site (Y397) (69). This signaling cascade leads to phosphorylation of several proteins including paxillin and other sites on FAK itself (53). Following one-hour B16/GPR4 cell attachment assays at pH 6.4, the localization was similar to that of phospho-paxillin (Y118) in that it was localized to the cell body and absent from the peripheral regions of the cell even when fully spread out (Figure 14A). At pH 6.4, 90% of the cells counted out of a total of 142 displayed a cell body localization of phospho-FAK (Y397) (Figure 14C). At pH 7.4, however, out of 135 B16/GPR4 cells counted, 18.5% of them were localized to the cell body with 81.5% localized to the cell periphery (Figure 14C). The percent of B16/Vector cells with a localization of phospho-FAK (Y397) in the cell periphery ranged from 84-94% at pH 6.4 and 7.4, and the percent cells that had localization in the cell body ranged from 7-16% (Figure 14C). The altered localization of phospho-FAK (Y397) seen in B16/GPR4 cells when treated with DMEM buffered to pH 6.4 was not seen in B16/Vector cells.

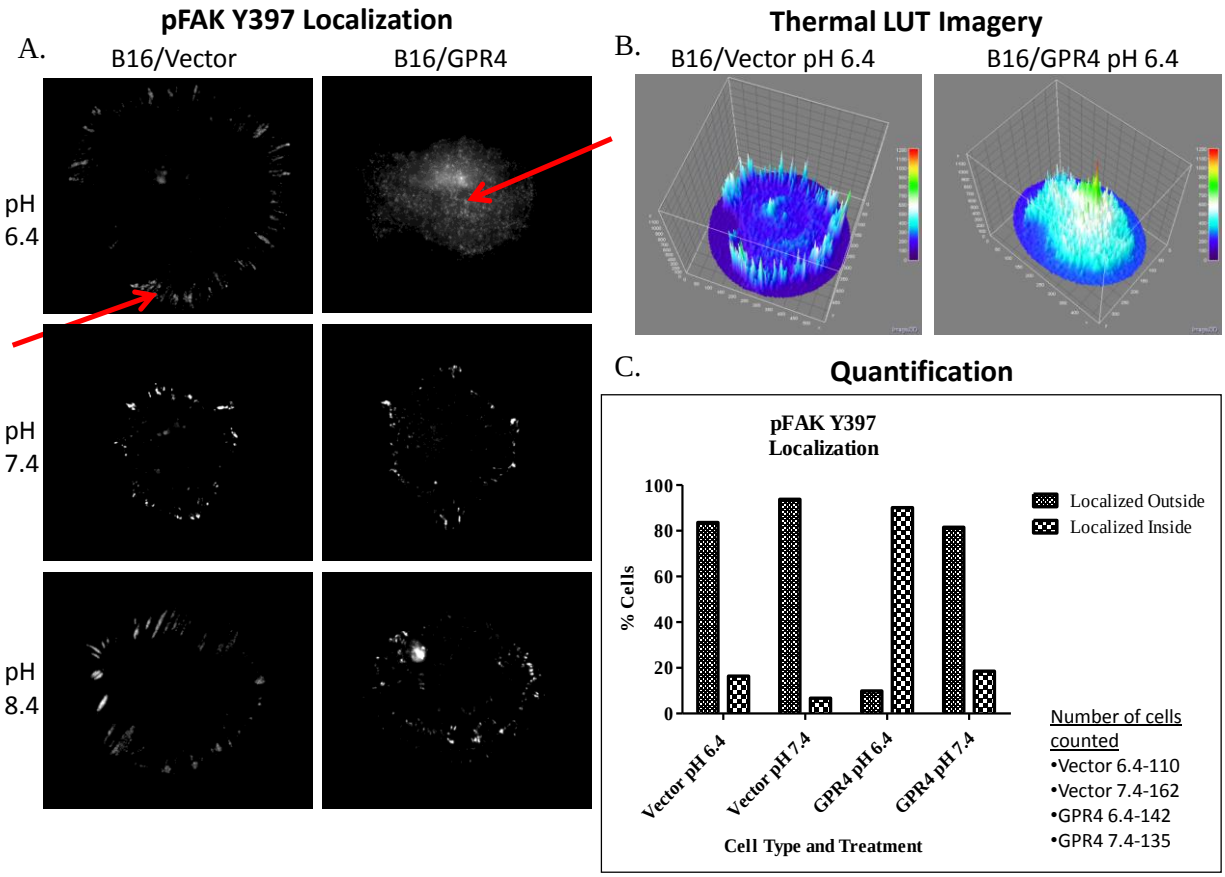

Figure 14. B16/Vector and B16/GPR4 Cell Phospho-Focal Adhesion Kinase (Y397) Immunocytochemsitry. (A) Localization of phospho-FAK (Y397) in B16/Vector and B16/GPR4 cells after a one-hour attachment to glass coverslips in DMEM buffered to pH 6.4, 7.4 or 8.4. (B) A surface plot of the emission signal using Thermal LUT, which displays the localization of phospho-FAK (Y397) in B16/Vector and B16/GPR4 cells. (C) Quantification of cell body (inside) or peripheral localization (outside) of phospho-FAK (Y397). Repeated 3 times.

Activation of GPR4 Alters Migrating Cell Morphology and Dynamics

Previously, GPR4 activation has been reported to inhibit cell migration by using cell culture wound closure assays and cell invasion by using transwell cell migration and invasion assays (15). To visualize the difference of B16/GPR4 cell migration in media buffered to pH 6.4 and 7.4 or when compared to the B16/Vector control cells, time-lapse cell culture wound closure assays were performed (Figure 15A-15D). The videos that were created following time-lapse cell culture wound closure assays at pH 6.4 and 7.4 allowed for the visualization of B16F10 melanoma cell migration velocity (98). The B16/Vector cells exhibited rapid migration at pH 6.4 and 7.4 where the wound was completely closed at the 12-hour mark (Figure 15A and 15B). Alternatively, B16/GPR4 cell migration was inhibited at pH 6.4 and did not close after 16 hours (Figure 15C) (98). Furthermore, individual cell migration was studied in detail using the videos generated by time-lapse photography (Figure 16A and B). B16/Vector cells exhibited highly dynamic cell migration and movement on the surface of the well. This facilitated the efficient closure of the wound after 12 hours (Figure 15A). B16/GPR4 cells, however, exhibited multiple defects that contributed to inhibited cell migration. In numerous B16/GPR4 cells there were several extensions (lamellipodia) that projected into opposing directions seemingly altering cell migration (Figure 16B). The trailing edge of the cell was also not able to detach generating an elongated trailing edge, which also inhibited cell migration (Figure 16B).

The inhibition of B16/GPR4 cell migration when treated with acidic media has been demonstrated in previous studies (15), but the restoration of migration has not yet been investigated. To recapitulate the migratory phenotype seen in B16/Vector cells at pH 6.4, the B16/GPR4 $G_{12/13}$- cell line was used to test the $G_{12/13}$ G-protein's involvement in reduced cell migration found in B16/GPR4 cells. Following quantification of B16/GPR4 $G_{12/13-}$ cell culture

wound closure assays at pH 6.4 cell migration was restored back to pH 7.4 and 8.4 treatment groups of B16/GPR4 cells (Figure 17A and 17B). The restoration of cell migration found in B16/GPR4 $G_{12/13}$- cells when treated with media buffered to pH 6.4 demonstrates that activation of GPR4 and subsequently the $G_{12/13}$ downstream pathway may be responsible for reduced cell migration.

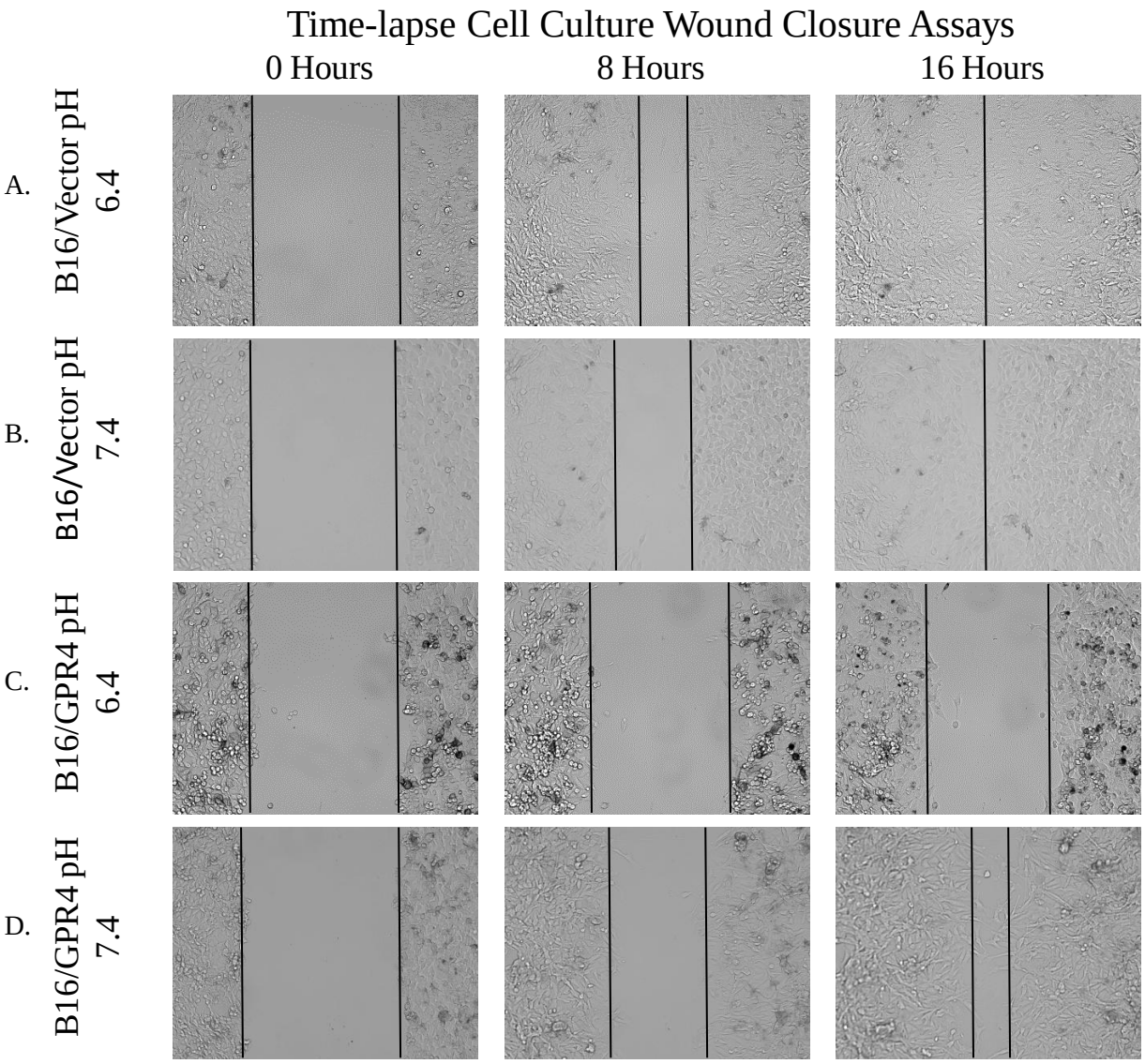

Figure 15. B16/Vector and B16/GPR4 Cell Time Lapse Cell Culture Wound Closure Assays. (A) B16/Vector, pH 6.4. (B) B16/Vector, pH 7.4. (C) B16/GPR4 pH 6.4. (D) B16/GPR4, pH 7.4.

A. B16/Vector B. B16/GPR4

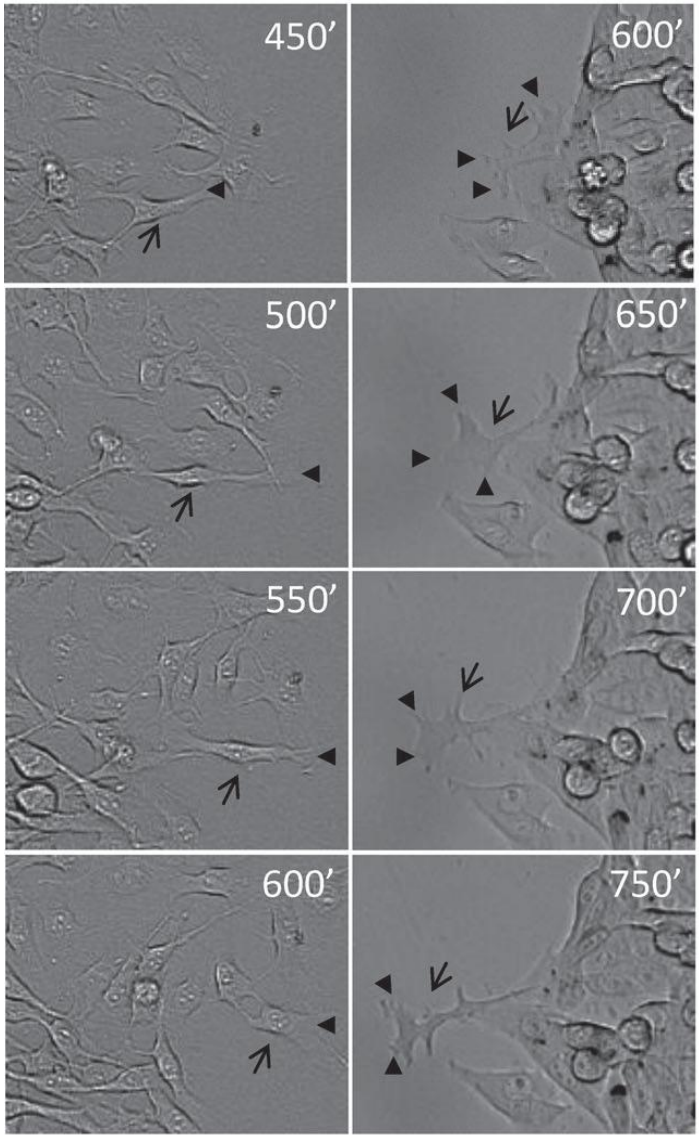

Figure 16. Activation of GPR4 Alters Individual B16/GPR4 Cell Migration During Cell Culture Wound Closure Assay. (A) The phase contrast images of the migrating B16/Vector and (B) B16/GPR4 cells at different times (in minutes) after the wounds were generated (Figure 15A and C). Arrows indicate representative migrating cells and arrowheads indicate lamellipodia (leading edge) of migrating cells. Please note the divergent lamellipodia and the elongated trailing edge of B16/GPR4 cells.

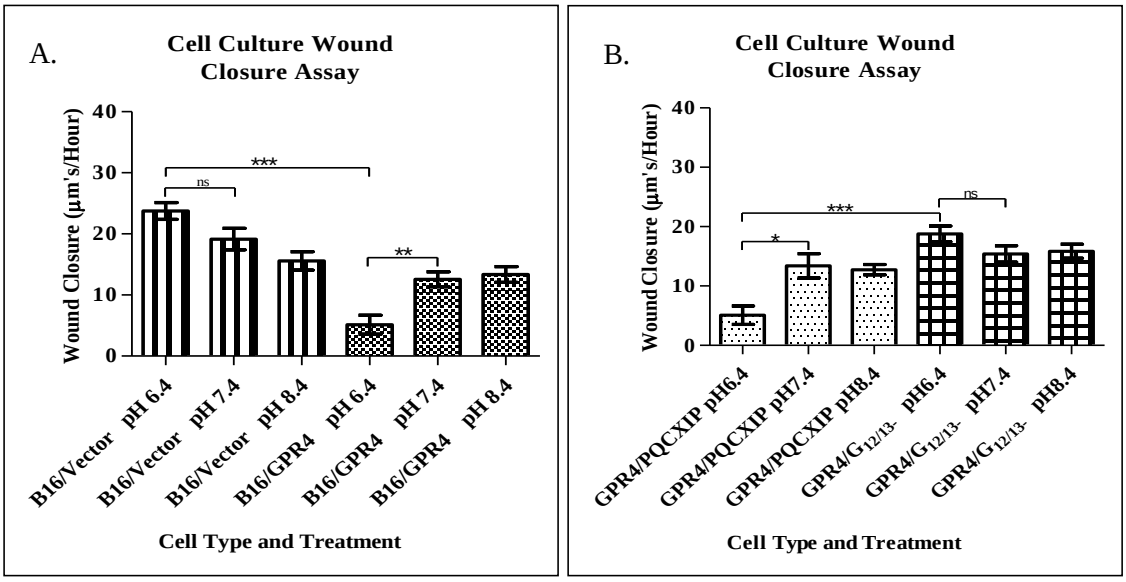

Figure 17. $G_{12/13}$ Signaling in B16/GPR4 Cell Quantitative Snapshot Cell Culture Wound Closure Assays. (A) B16/Vector and B16/GPR4 cell snapshot cell culture wound closure assay at pH 6.4, 7.4, and 8.4. (B) B16/GPR4 PQCXIP and B16/GPR4 $G_{12/13-}$ cell snapshot cell culture wound closure assay at pH 6.4, 7.4, and 8.4. Please note restored B16/GPR4 cell migration at pH 6.4. Each treatment group consisted of 6-13 repeats. (*** $P < .001$, ** $P < .01$, * $P < .05$, ns $P > .05$)

Activation of GPR4 Alters Phospho-Paxillin (Y118) Localization in Spontaneously Migrating B16/GPR4 Cells

To further investigate areas of dynamic nature, i.e. areas with a high focal adhesion turnover rate, in B16/GPR4 cells at pH 6.4 we investigated phospho-paxillin (Y118) localization in spontaneously migrating cells. It was previously demonstrated that the localization of phospho-paxillin (Y118) and phopho-FAK (Y397) is altered in B16/GPR4 cells during attachment and spreading at pH 6.4 (Figure 13 and 17). Moreover, following cell culture wound closure assays it was also established that the B16/GPR4 cells were having trouble migrating partially due to delayed trailing edge detachment (Figure 15) (98). To determine what mechanism is reducing trailing edge detachment in B16/GPR4 cells phospho-paxillin (Y118) localization was investigated due to its ability to localize to newly formed and deteriorating focal adhesions. Next, immunocytochemistry of phospho-paxillin (Y118) was performed and cells that were spontaneously migrating were selected for photographs. Pictures were taken at 100X, 200X, and 1000X total magnification of several B16/Vector and B16/GPR4 cell samples. The results demonstrated that there was an alteration in the localization of phospho-paxillin (Y118) in migrating B16/GPR4 cells when treated with DMEM buffered to pH 6.4. The leading edge of the B16/Vector cells demonstrated an accumulation of phospho-paxillin (Y118) as well as an accumulation in the trailing edge region where detachment occurs (Figure 18A). In B16/Vector cells, 87% of the cells counted localized phospho-paxillin (Y118) to the leading edge and trailing edge region and 13% was missing its accumulation at the leading edge or trailing edge region (Figure 18B). B16/GPR4 cells, however, had a reduction in the accumulation of phospho-paxillin (Y118) (12%) at the leading edge and at the trailing edge region (Figure 18B). This indicates that there may be an absence of dynamic focal adhesions in these regions when GPR4

is active. The absence of newly formed or breaking down focal adhesions at these sites may impair B16/GPR4 cell migration due to the aberrant maturation of focal adhesions and reduced focal adhesion turnover.

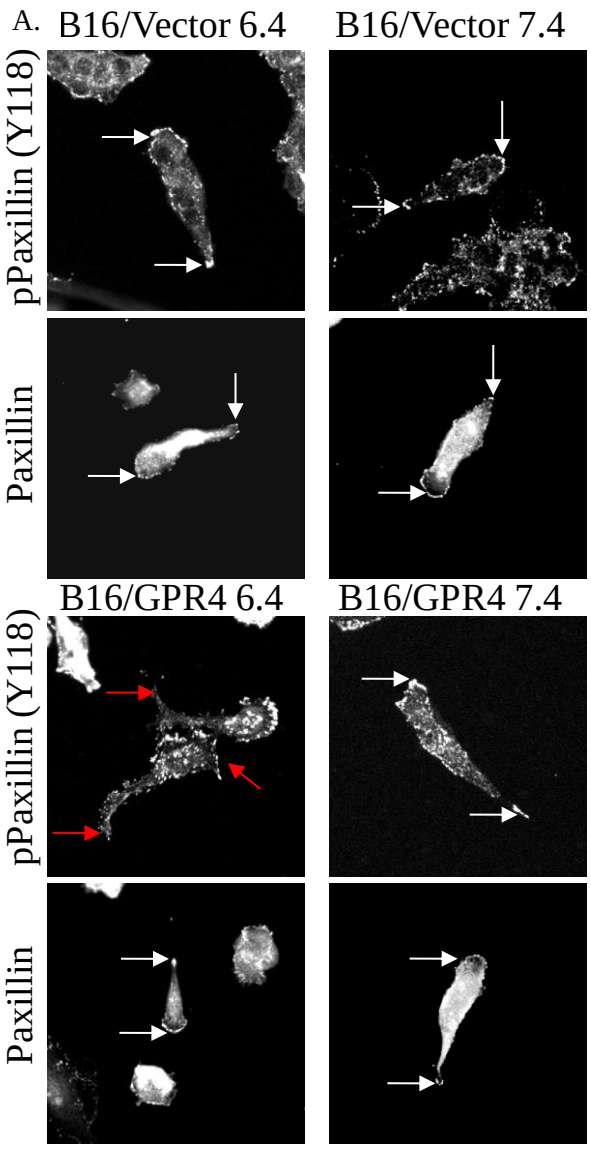

B.

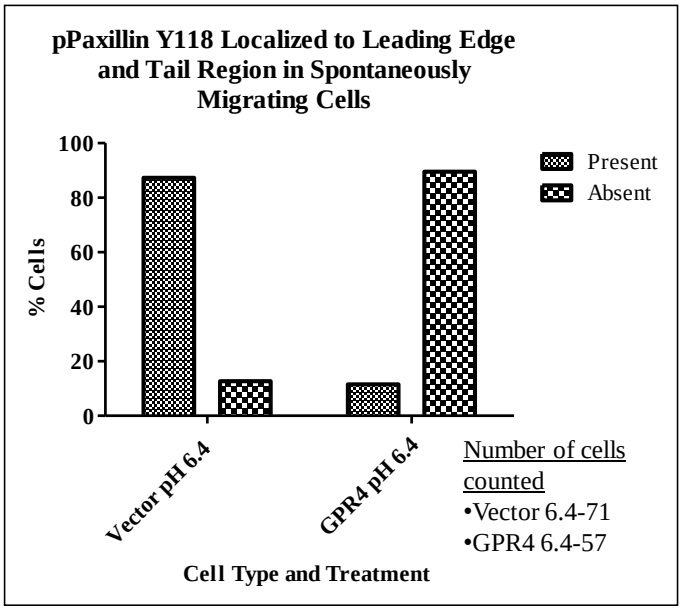

Figure 18. Migrating B16/Vector and B16/GPR4 Cell Phospho-Paxillin (Y118) and Total Paxillin Immunocytochemistry. (A) Migrating B16/Vector and B16/GPR4 cell total paxillin and phospho-paxillin (Y118) ICC at pH 6.4 and 7.4. Please note the white arrows pointing to normal transient focal adhesions in the leading edge and trailing edge region and red arrows pointing to the lack of transient focal adhesions in these areas. The lack of transient focal adhesions in the trailing edge region most likely contributes to a characteristic elongated trailing edge in B16/GPR4 cells (Figure 16B). (B) Migrating B16/Vector and B16/GPR4 cell phospho-paxillin (Y118) quantitative ICC. Repeated 2 times.

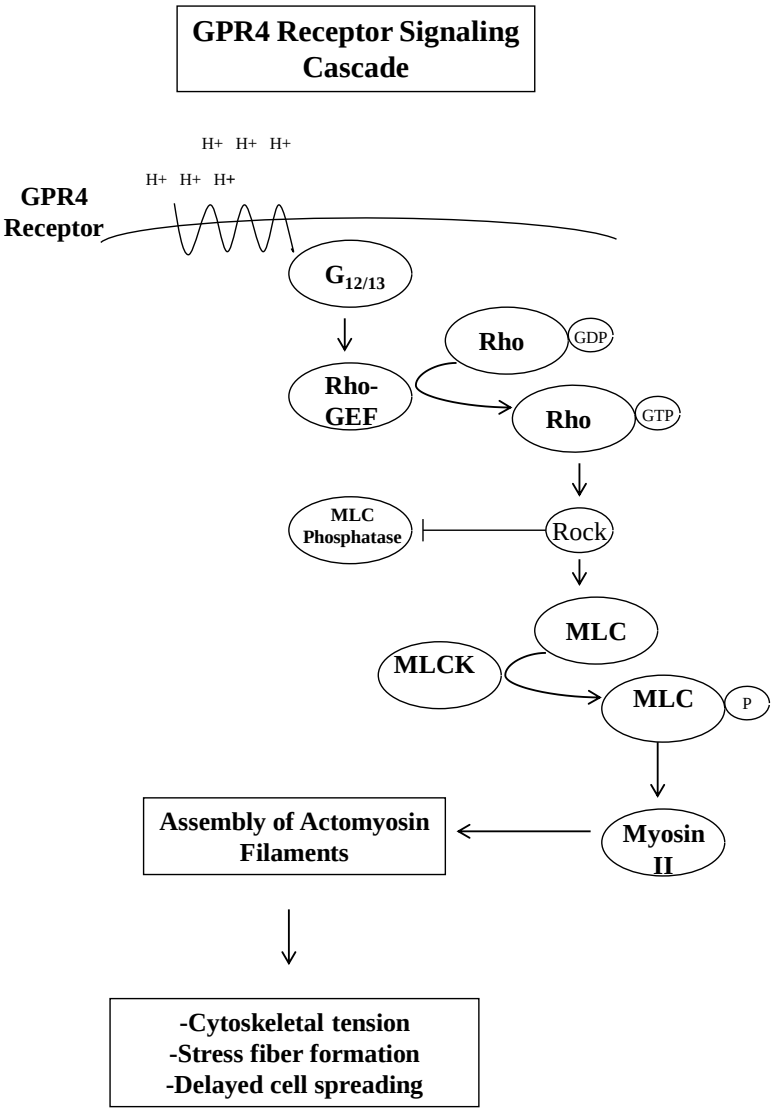

Diagram 6. Hypothesized GPR4 Signaling Cascade Diagram

Chapter 4: Discussion

In this study we examined the effects of GPR4 activation on B16F10 melanoma cell attachment, spreading, and migration. In addition, we explored the potential molecular mechanism that may be the foundation for reduced metastatic potential found previously in B16/GPR4 cells (15). Several reports provide evidence for acidic environments to either enhance or reduce the migration and metastatic capabilities of tumor cells (15, 31, 58, and 61). The migration and invasive ability of B16/GPR4 cells has been studied previously, but delayed cell spreading was not investigated. The signaling mechanisms that delay cell spreading following GPR4 activation in B16/GPR4 melanoma cells may further explain the effects of an acidic microenvironment on primary tumor cells. Furthermore, the importance of cell spreading in circulating cancer cell survival is high and by activating the $G_{12/13}$ G-protein signaling pathways possibly with chemicals that were used in this study (CN01) or by introducing the GPR4 construct to a primary tumor site we may add to the numerous therapeutic strategies used to treat cancer (54 and 68).

At acidic pH, the attachment and spreading of B16F10 melanoma cells that express GPR4 at a high level is delayed in comparison to the vector control B16 cells when plated on several substrates (Figures 2 and 3). Viewed by time-lapse attachment assays in vitro, the dynamic movements typically found in B16F10 melanoma cells has been lost following the aberrant expression of GPR4 (98). This may also correlate with previous results that report reduced B16/GPR4 cell pulmonary metastasis in mice post tail vein injections (15). Moreover, the reduction in membrane protrusions in B16/GPR4 cells during attachment and spreading and while suspended may also further verify the report that increased micro-metastatic outgrowth may be facilitated by filopodia-like structures (68 and 98). We also demonstrate that activation

of GPR4 is coupled to the $G_{12/13}$ G-protein and that its activity possibly delays cell spreading and further reduces the number of membrane protrusions because of increased cytoskeletal tension and membrane rigidity.

Established in several reports, cytoskeletal tension must be relieved during the initial phase of cell spreading (5 and 86). Furthermore, cell spreading is reportedly inversely correlated with myosin activity (5 and 86). The small molecule Rho is partially responsible for facilitating myosin activity and is downstream from the $G_{12/13}$ G-protein (39). This is particularly relevant to this study due to previous results that demonstrate an increase in Rho activation in B16/GPR4 cells when compared to B16/Vector cells at pH 6.4 (15). The increased activity of Rho also correlated with increased actin stress fiber development in B16/GPR4 cells when serum starved and treated with media buffered to pH 6.4 (15). Furthermore, when B16/GPR4 $G_{12/13}$- cells are serum starved and treated with media buffered to pH 6.4 actin stress fiber development is absent (Figure 7E). This correlates with restored cell spreading following a one-hour attachment assay (Figure 7A). To further examine delayed B16/GPR4 cell spreading CT04 was used to inhibit Rho activation during a one-hour attachment assay. The inhibition of Rho with CT04 in B16/GPR4 cells restored cell spreading, which indicates Rho's involvement in B16/GPR4 cell spreading (Figure 6A). Increased intensity of Rho-mediated actomyosin contractility has been demonstrated in several reports to reduce membrane protrusions and delay cell spreading and migration (5 and 23). This hypothesis may potentially explain why B16/GPR4 cell spreading is delayed at pH 6.4.

Downstream of Rho activation is the activation of the Rho kinase (ROCK). Rho and ROCK has been reported to phosphorylate the MBS site of MLC-phosphatase, which leads to its deactivation (25 and 37). Inactivation of MLC-phosphatase by ROCK increases the relative

phosphorylation of MLC indirectly. ROCK has also been reported to phosphorylate MLC directly in vitro, which increases cytoskeletal tension and may produce actin stress fibers that are similar to B16/GPR4 cells at pH 6.4 (Figure 3D) (81). Next, the hypothesis that Rho activation may increase ROCK activation and subsequently stimulate MLC phosphorylation in B16/GPR4 cells was investigated. During a one-hour attachment assay at pH 6.4 B16/GPR4 cells were treated with Y27632 and its function restored their ability to spread (Figure 9A). What's more, following serum starvation for two days and cytoskeletal staining using Rhodamine phalloidin actin stress fibers were absent in B16/GPR4 cells at pH 6.4 when treated with Y27632 (Figure 9D). To examine the possible effects of reduced myosin light chain (MLC) phosphorylation on the ability of B16/GPR4 cells to spread, staurosporine (STA) was used to inhibit myosin light chain kinase (MLCK) activity during a one-hour attachment assay. Following the inhibition of MLCK by STA, B16/GPR4 cell spreading was restored (Figure 9B). Moreover, after serum starvation for two days and treatment with STA for one hour at pH 6.4 actin stress fibers were absent (Figure 9E). These results support the premise that GPR4/$G_{12/13}$/RHO/ROCK activation may directly or indirectly activate MLC and lead to increased cytoskeletal tension and delayed B16/GPR4 cell spreading at pH 6.4.

B16/Vector and B16/GPR4 cell spreading and the G-protein signaling pathways responsible for the effects at acidic pH were investigated thoroughly in this report but as with any study there were limitations. To begin, there was no direct observation that round B16/GPR4 cells had increased myosin contractility at pH 6.4; only that actin stress fiber development was present in the same conditions while cells were spread on a surface (Figure 3D). In addition, the activation of $G_{12/13}$ was never measured directly but was assumed active due to the restoration in B16/GPR4 cell spreading following the application of a $G_{12/13}$ inhibitory construct (Figure 7A).

Furthermore, the activity of Rho, cAMP levels, ROCK activity, MLCK activity, and cytosolic calcium levels were never directly measured following the use of chemicals that were theoretically believed to lead to the manipulation of these pathways, e.g. CT04, CN01, 8-bromo-cAMP, DDA, Y27632, staurosporine, and thapsigargin. As for the $G_{12/13}$ and G_q G-protein pathways, the inhibitory constructs that were used made up for this limitation. However, the G_s pathway was not inhibited with a transduced construct, which was a limitation in the investigation of G_s signaling.

GPR4 signaling that leads to delayed cell spreading has been discussed and the potential mechanism responsible for these effects has potentially been unveiled. Although the mechanism following activation may have been indirectly uncovered, the effects on focal adhesion formation and cell migration have not yet been examined in detail. In several reports phospho-paxillin (Y118) has been demonstrated to localize to dynamic focal adhesions (5, 91, and 97). The localization of phospho-FAK (Y397) may also represent dynamic focal adhesions. When it is present at regions of integrin clustering it may recruit SRC and may allow for focal adhesion turnover. Several reports cite the presence of SRC may facilitate the degradation of focal adhesions (30 and 91). Furthermore, focal adhesion turnover also occurs through the calcium dependent protease calpain (14, 30, and 72). Calpain's interaction with FAK is required for the calpain-mediated disassembly of focal adhesions, which may increase focal adhesion turnover (14 and 30). Dynamic focal adhesions have a high turnover rate and are in the continuous process of either being assembled or disassembled. Cells that contain a high number of transient focal adhesions may also migrate and spread faster. Alternatively, mature focal adhesions lack (Y118) phosphorylated paxillin and exhibit reduced turnover rates, which may reduce membrane ruffling and cell migration (5, 91, and 97). To investigate the localization of dynamic adhesions

in B16/GPR4 cells at pH 6.4 during cell spreading, cells were immuno-stained with a phospho-paxillin (Y118) or phospho-FAK (Y397) antibody after a one-hour attachment assay on glass coverslips. The results reveal an alteration in the localization of phospho-paxillin (Y118) and phospho-FAK (Y397) from the cell periphery to the cell center (Figure 13 and 17). The altered localization of dynamic focal adhesions from the B16/GPR4 cell periphery to the center correlates with the reduction in membrane ruffling previously viewed by time-lapse photography (98). The $G_{12/13}$/Rho/ROCK/MLC mechanism influencing cell spreading discussed previously may also be correlated with these changes (Diagram 6). ROCK activation in several studies has been reported to alter the localization of focal adhesions to the cell center from the cell periphery and may also encourage an amoeboid like morphology (62, 80, and 81). Furthermore, constitutively active MLC due to inhibited MLC phosphatase activity can also lead to inhibited migration because of reduced focal adhesion turnover and focal adhesion maturation (80). As the localization of dynamic focal adhesions is altered in B16/GPR4 cells at pH 6.4 total paxillin was not altered and did not show any variation when compared to pH 7.4 or B16/Vector cells (Figure 13). This indicates that stable focal adhesions were present but dynamic focal adhesions were absent in areas that permit efficient membrane ruffling.

Following the investigation of B16/GPR4 cell spreading and focal adhesion dynamics at pH 6.4, cell migration was examined next. In previous studies B16/GPR4 cell migration in vitro was inhibited (15). In this study time-lapse and quantitative cell culture wound closure assays were used to examine the morphological characteristics and velocity of migrating B16F10 cells. B16/GPR4 cell migration appeared to be inhibited at pH 6.4 and also exhibited an elongated trailing edge due to an inability to detach (Figure 15C, 16B, and 17A) (98). To investigate the signaling pathways that may lead to inhibited B16/GPR4 cell migration at pH 6.4 B16/GPR4

$G_{12/13-}$ and B16/GPR4 PQCXIP cells were used in cell culture wound closure assays (Figure 17B). Following quantification of B16/GPR4 $G_{12/13-}$ cell wound closure there was a significant rescue of cell migration (Figure 17B). Furthermore, cell migration does not seem to fluctuate as it did before when exposed to media buffered to pH 6.4, 7.4, or 8.4 (Figure 17B). This validates that GPR4 signaling through the $G_{12/13}$ G-protein signaling pathway inhibits B16/GPR4 cell migration (Figure 17B).

As we studied the activation of GPR4 in B16/GPR4 cells and found that cell migration was reduced at acidic pH, we also found other effects of acidosis on B16/Vector cell migration. In Figure 2A, 3C, 5C, 15A, and 17A the B16/Vector cell migration velocity and the migrating cell percentage was increased at pH 6.4. When comparing B16/Vector cells with B16/GPR4 cells at pH 6.4 the effects on cell migration seem to be the opposite. The migration velocity and migrating B16/GPR4 cell percentages were reduced at pH 6.4. As the expression level of GPR4 in B16/Vector cells are relatively low, this may represent the response of a cell without proton-sensing G-protein coupled receptor expression to acidosis. In one known report OGR1 overexpression was reduced in distant metastasis in comparison to the primary tumor site, which may imply that the proton-sensing G-protein coupled receptors may function as metastasis suppressor genes (41 and 70).

Discussed in detail previously was focal adhesion dynamics during B16F10 cell spreading. After accepting that there was an alteration in the localization of dynamic focal adhesions during B16/GPR4 cell spreading when treated with media buffered to pH 6.4 we hypothesized that there was a potential connection between altered focal adhesion dynamics and inhibited B16/GPR4 cell migration. To test this hypothesis we immuno-stained B16/GPR4 cells with phospho-paxillin (Y118) and total paxillin twenty-four hours after plating to permit efficient

time for cell spreading and spontaneous migration. The results demonstrate that not only was there an alteration in focal adhesion dynamics during B16/GPR4 cell spreading at pH 6.4 but the localization of dynamic focal adhesions in migrating cells were altered as well (Figure 18A). In normal migrating cells dynamic focal adhesions are localized to the leading edge and the trailing edge of the cell to allow for efficient migration. On the other hand, in the event that dynamic focal adhesions are not localized to these regions cell migration may be disrupted. The dynamic focal adhesion localization in B16/GPR4 cells when treated with media buffered to pH 6.4 seemed to be throughout the cell in unusual regions that they are not normally found (Figure 18A). There was also an absence of dynamic focal adhesions in the leading edge as well as the trailing edge region, which potentially explains reduced trailing edge detachment, previously viewed in time-lapse cell culture wound closure videos (Figure 18A-B) (98). Various reports indicate that constitutively active MLC may lead to the stabilization of focal adhesions and may also block cell migration, which is also true of Rho and ROCK (17 and 80). As discussed previously paxillin is localized in mature focal adhesions. In spontaneously migrating B16/GPR4 cells paxillin is present in dynamic regions such as the leading edge and trailing edge but phospho-paxillin (Y118) is not (Figure 18). This demonstrates the absence of transient focal adhesions but presence of mature focal adhesions in B16/GPR4 cells at pH 6.4. The alteration of focal adhesion dynamics in B16/GPR4 cells may be potentially connected to a GPR4/$G_{12/13}$/Rho/ROCK/MLC signaling pathway (Diagram 6) that when constitutively active will lead to the aberrant maturation of focal adhesions, which could lessen cell migration.

The results that were obtained in this study have promise for future investigation of GPR4 or other proton sensing G-protein coupled receptors in the process of tumor cell invasion and metastasis. Following the overexpression of GPR4 in B16F10 melanoma cells cell spreading

was delayed and their normal dynamic nature was lost potentially due to increased cytoskeletal tension and membrane rigidity. Reducing membrane protrusions and losing the dynamic nature of the cell membrane may reduce the chances for a tumor cell to invade tissue and enter the blood stream (68). It may also diminish the possibility of circulating cancer cells to attach and invade a distant tissue. Previously unknown data about GPR4 signaling has also been uncovered such as GPR4 signaling specifically through $G_{12/13,}$ Rho, ROCK, and MLC pathway (Diagram 6) to increase cytoskeletal tension. In addition, GPR4 signaling may also alter focal adhesion dynamics. $G_{12/13}$ signaling potentially explains several of the effects seen in B16/GPR4 cells following the stimulation of GPR4 by acidic media. Furthermore, as focal adhesion dynamics, cell spreading, and cell migration are important for a broad range of physiological processes the alteration in cell dynamics following GPR4 activation may have future potential in various fields of research.

The potential implications for this study may be advantageous in the management of tumor metastasis as this field is in need of new treatment options. There may be an avenue for chemical therapy that exists based on targeting certain aspects of the tumor microenvironment. In particular acidosis may be used to target drug release to reduce the systemic effects commonly observed when utilizing chemical therapy to treat cancer (44 and 99). Furthermore, gene therapy that commonly detects unwanted systemic toxicity may be used with further efficacy with approaches that target tumor acidosis (44 and 99). Several reports have investigated the potential to target drugs to the acidic microenvironment. One such method established that by using polyethylene glycol (PEG)-based hydrogels integrated with Imidazole that drug release (Antagomir) was enhanced in acidic environments (44). Imidazole is a heterocyclic organic compound that may accept protons and allows for increased water solubility and enhanced

degradation of PEG-based hydrogels (44). As Antagomir may be released efficiently in acidic environments, additional efficacious materials that induce anti metastatic responses may be used as well. For example, introducing plasmid DNA, such as the MSCV-huGPR4-IRES-GFP vector used in this study, into PEG-based hydrogels may potentially be developed in the future. Equivalent to targeting acidosis in the tumor microenvironment by using PEG-based hydrogels is incorporating chemical drugs in liposomes that are degraded through acid sensitive mechanisms (99). Moreover, a drug or antibody carried by nanoparticles that may potentiate GPR4 activation may induce a response in tumor cells that is similar to this report for example: delayed cell spreading, inhibited migration, and altered focal adhesion dynamics. The therapeutic implications for tumor cell response to the acidic microenvironment by the proton sensing G-protein coupled receptors seem ample as there is a broad range of potential therapeutic discoveries still to be established in this family.

In conclusion, the implications for cancer therapy have been discussed but relevance of the proton sensing G-protein coupled receptors in normal cells is still not been completely understood. It is most likely highly expressed in the areas of the human body that need a delicate pH balance, e.g. kidney, lung, or other tissue that regulates acid-base balance. Furthermore, there is little known about the expression levels of the proton sensing G-protein coupled receptors throughout the extremely large variety of human cancers. Unpublished data in Dr. Yang's lab has uncovered a higher expression of these receptors in hematological malignancies such as leukemia and lymphomas. This relatively unexplored family of proton sensing G-protein coupled receptors is an extremely new aspect of study in cancer research and in normal physiological function. The avenues for research on this topic are ever-expanding and may even further our general knowledge of cell biology and human disease.

References

1) Alberts, B. et al. Molecular Biology of the Cell (5th Edition). Garland Science, Taylor and Francis Group, LLC, 2008. Print

2) American Cancer Society (2012). Cancer Facts and Figures 2012. Atlanta, Georgia: American Cancer Society Inc

3) Amano, M., Chihara, K., Kimura, K., Fukata, Y., Nakamura, N., Matsuura, Y., Kaibuchi, K. (1997). Formation of Actin Stress Fibers and Focal Adhesion Enhanced by Rho-Kinase. *Science* 275 (5304): 1308-1311

4) Arora, A. and Scholar, E. M. (2005). Role of Tyrosine Kinase Inhibitors in Cancer Therapy. *The Journal of Pharmacology and Experimental Therapeutics* 315: 3: 971-979

5) Arthur, T. and Burridge, K. (2001). RhoA Inactivation by p190RhoGAP Regulates Cell Spreading and Migration by Promoting Membrane Protrusion and Polarity. *Molecular Biology of the Cell* 12: 2711-2720

6) Barrallo-Gimeno, A., Nieto, M. A. (2005). The Snail genes as inducers of cell movement and survival: implications in development and cancer. *Development* 132: 3151–3161

7) Beierle, E. A., Ma, X., Stewart, J., Nyberg, C., Trujillo, A., Cance, W. G., Golubovskaya, V. M. (2010). Inhibition of Focal Adhesion Kinase Decreases Tumor Growth in Human Neuroblastoma. *Cell Cycle* 9: 5: 1005-1015

8) Bendas, G. and Borsig, L. (2012). Cancer Cell Adhesion and Metastasis: Selectins, Integrins, and the Inhibitory Potential of Heparins. *International Journal of Cell Biology*

9) Blackburn E. H. (1991). Structure and Function of Telomeres. *Nature* 350: 569-573

10) Boedtkjer, E., Bunch, L., Pedersen, S. F. (2012). Physiology, pharmacology and pathophysiology of the pH regulatory transport proteins NHE1 and NBCn1: Similarities, differences, and implications for cancer therapy. *Current Pharmaceutical Design* 18(10): 1345-71

11) Brown, M. C., West, K. A., Turner, C. E. (2002). Paxillin-dependent Paxillin Kinase Linker and p21-Activated Kinase Localization to Focal Adhesions Involves a Multistep Activation Pathway. *Molecular Biology of the Cell* 13: 5: 1550-1565

12) Burridge, K. and Doughman, R. (2006). Front to back by Rho and Rac. *Nature Cell Biology* 8: 8: 781-782

13) Carman, C. V., Parent, J. L., Day, P. W., et al. (1999). Selective regulation of Gα (q/11) by an RGS domain in the G protein–coupled receptor kinase, GRK2. *The Journal of Biological Chemistry* 274: 34483-34492

14) Carragher, N. O., Westoff, M. A., Finchham, V. J., Schaller, M. D., Frame, M. C. (2003). A Novel Role for FAK as a Protease-Targeting Adapter Proteins: Regulation by p42 ERK and Src. *Current Biology* 19: 13(16): 1442-1450

15) Castellone, R., Leffler, N., Dong, L., Yang, L. (2011). Inhibition of Tumor Cell Migration and Metastasis by the Proton-Sensing GPR4 Receptor. *Cancer Letters* 312: 2: 197-208

16) Chaffer, C. L. and Weinberg R. A. (2011). A Prospective on Cancer Cell Metastasis. *Science* 331: 1559

17) Chen, B-H., Tzen, J. T. C., Bresnick, A. R., Chen, H-C. (2002). Roles of Rho-associated Kinase and Myosin Light Chain Kinase in Morphological and Migratory Defects of Focal Adhesion Kinase-Null Cells. *The Journal of Biological Chemistry* 277: 37: 33857-33863

18) Chen, J. L-Y., Lucas, J. E., Schroeder, T., Mori, S., Wu, J., Nevins, Dewhirst, M., West, M., Chi, J-T. (2008). The Genomic Analysis of Lactic Acidosis and Acidosis Response in Human Cancers. *PLoS Genetics* 4: 12: e1000293

19) Cheng, Z., Garvin, D., Paguio, A., Stecha, P., Wood, K., Fan, F. (2010). Luciferase Reporter Assay System for Deciphering GPCR Pathways. *Current Chemical Genomics* 4: 84–91

20) Cooper, J. A. and Schafer D. A. (2000). Control of Actin Assembly and Disassembly at Filament Ends. *Current Opinion in Cell Biology* 12: 97-103

21) Dalerba, P., Cho, R. W., Clarke, M. F. (2007). Cancer Stem Cells: Models and Concepts. *Annual Review of Medicine* 58: 267-284

22) Enerson, B. E. & Drewes, L. R. (2003). Molecular features, regulation, and function of monocarboxylate transporters: implications for drug delivery. *Journal of Pharmaceutical Sciences* 92: 1531–1544

23) Flevaris, P., Stojanovic, A., Gong, H., Chrishti, A., Welch, E., Du, X. (2007). A Molecular Switch that Controls Cell Spreading and Retraction. *The Journal of Cell Biology* 179: 3: 553-565

24) Fredriksson, R. and Schiöth, H. B. (2005). The Repertoire of G-Protein-Coupled Receptors in Fully Sequenced Genomes. *Molecular Pharmacology* 67: 5: 1414-1425

25) Fukata, M., Nakagawa, M., Kuroda, S., Kaibuchi, K. (1999). Cell Adhesion and Small Rho-GTPases. *Journal of Cell Science* 112: 4491-4500

26) Gout, S., Tremblay, P., Huot J. (2008). Selectins and Selectin Ligands in Extravasation of Cancer and Organ Selectivity of Metastasis. *Clinical Experimental Metastasis* 25: 335-344

27) Greaves, M., Maley, C. (2012). Clonal Evolution in Cancer. *Nature* 481: 306-313

28) Griffiths, J. R. (1991). Are cancer cells acidic? *British Journal of Cancer* 64: 425-427

29) Halestrap, A. P. & Price, N. T. (1999). The proton-linked mono-carboxylate transporter (MCT) family: structure, function and regulation. *Biochemical Journal* 343: 281–299

30) Hamadi, A., Bouali, M., Dontenwill, M., Stoeckel, H., Takeda, K., Ronde, P. (2005). Regulation of Focal Adhesion Dynamics and Dissasembly by Phosphorylation of FAK at Tyrosine 397. *Journal of Cell Science* 118: 4415-4425

31) Hanahan, D. and Weinberg, R. A. (2011). Hallmarks of Cancer: The Next Generation. *Cell* 144: 646-674

32) Hanahan, D. and Weinberg, R. A. (2000). The Hallmarks of Cancer. *Cell* 100: 1: 57-70

33) Hauck, C. R., Hsia, D. A., Puente, X. S., Cheresh, D. A. and Schlaepfer, D. D. (2002). FRNK blocks v-Src-stimulated invasion and experimental metastases without effects on cell motility or growth. *EMBO Journal* 21: 6289-6302

34) Hauck, C. R., Sieg, D. J., Hsia, D. A., Loftus, J. C., Gaarde, W. A., Monia, B. P. and Schlaepfer, D. D. (2001). Inhibition of focal adhesion kinase expression or activity disrupts epidermal growth factor-stimulated signaling promoting the migration of invasive human carcinoma cells. *Cancer Research* 61: 7079-7090

35) Hynes, R. (2002). Integrins: Bidirectional Allosteric Signaling Machines. *Cell* 110: 673-687

36) Ibrahim-Hashim, A., Cornell, H. H., Abrahams, D., Lloyd, M., Bui, M., Gillies, R. J. Gatenby, R. A. (2012). Systemic Buffers Inhibit Carcinogenesis in TRAMP Mice. *The Journal of Urology* 188: 2: 624-631

37) Kimura, K., Amano, M., Chihara, K., Fukata, Y., Nakafuku, M., Yamamori, B., Feng, J., Nakano, T., Okawa, K., Iwamatsu, A., Kaibuchi, K. (1996). Regulation of Myosin Phosphatase by Rho and Rho-Associated Kinase (Rho-Kinase). *Science* 12: 273(5272): 245-248

38) Kirichok, Y., Krapivinsky, G., Clapham, D. E. (2004). The Mitochondrial Calcium Uniporter is a Highly Selective Ion Channel. *Letters to Nature* 427: 360-364

39) Kozasa, T., Jiang, X., Hart, M. J., et al. (1998). p115 RhoGEF, a GTPase activating protein for Gα12 and Gα13. *Science* 280: 2109-2111

40) Lagadic-Gossmann, D., Huc, L. and Lecureur, V. (2004). Alterations of Intracellular pH Homeostasis in Apoptosis: Origins and Roles. *Cell Death and Differentiation* 11: 953–961

41) LaTulippe, E. , Satagopan, J. , Smith, A. , Scher, H. , Scardino, P. , Reuter, V. , et al. (2002). Comprehensive gene expression analysis of prostate cancer reveals distinct transcriptional programs associated with metastatic disease. *Cancer Research* 62: 4499–506

42) Lauffenburger, D. A., and Horwitz, A. F. (1996). Cell Migration: A Physically Integrated Molecular Process. *Cell* 84: 359–369

43) Ley, K., Laudanna, C., Cybulsky, M., Nourshargh, S. (2007). Getting to the Site of Inflammation: The Leukocyte Adhesion Cascade Updated. *Nature Reviews Immunology* 7: 678-689

44) Lin, C-W., Tseng, S-J., Kempson, I. M., Yang, S-C., Hong, T-M., Yang, P-C. (2012). Extracellular Delivery of Modified Oligonucleotide and Superparamagnetic Iron Oxide Nanoparticles from a Degradable Hydrogel Triggered by Tumor Acidosis. *Biomaterials* 34: 17: 4387-4393

45) Liu, Y., Loijens, J. C., Martin, K. H., Karginov, A. V. and Parsons, J. T. (2002). The association of ASAP1, an ADP ribosylation factor-GTPase activating protein, with focal adhesion kinase contributes to the process of focal adhesion assembly. *Molecular Biology of the Cell* 13: 2147-2156

46) Ludwig, M. G., Vanek, M., Guerini, D., Hasser, J. A., Jones, C. E., Junker, U., Hofstetter, H., Wolf, R. M., Seuwen, K. (2003). Proton-Sensing G-protein-Coupled Receptors. *Nature* 4: 425 6953: 93-98

47) Luzzy, K., MacDonald, I., Schmidt, E., Kerkvliet, N., Morris, V., Chambers, A., Groom, A. (1998). Multistep Nature of Metastatic Inefficiency. *American Journal of Pathology* 153: 3: 865-873

48) Maley, C. C., et al. (2004). Selectively advantageous mutations and hitchhikers in neoplasms: p16 lesions are selected in Barrett's esophagus. *Cancer Research* 64: 3414-3427

49) Marino, M. L., et al. (2012). Autophagy Is a Protective Mechanism for Human Melanoma Cells under Acidic Stress. *The Journal of Biological Chemistry* 287: 30664-30676

50) Matilla, P. K. and Lappalainen, P. (2008). Filopodia: Molecular Architecture and Cellular Functions. Nature Reviews: *Molecular Cell Biology* 9: 446-453

51) Matsuyama, S., Llopis, J., Deveraux, Q. L., Tsien, R. Y., Reed, J. C. (2000). Changes in Intramitochondrial and Cytosolic pH: Early Events that Modulate Caspase Activation during Apoptosis. *Nature Cell Biology* 2: 318–325

52) Orive, G., Reshkin, S. J., Harguindey, S., et al. (2003). Hydrogen Ion Dynamics and the Na^+/H^+ Exchanger in Cancer Angiogenesis and Antiangiogenesis. *British Journal of Cancer* 89: 1395-1399

53) Parsons, J. T. (2003). Focal Adhesion Kinase the First Ten Years. *Journal of Cell Science* 116: 1409-1416

54) Phipps, L. E., Hino, S., Muschel, R. (2011). Targeting Cell Spreading: A Method of Sensitizing Metastatic Tumor Cells to TRAIL-induced Apoptosis. *Molecular Cancer Research* 9: 249-258

55) Phan, G. Q., Messina, J. L., Sondak, V. K., Zager, J. S. (2009). Sentinel Lymph Node Biopsy for Melanoma: Indications and Rationale. *Cancer Control* 16: 3: 234-239

56) Polte, T. R. and Hanks, S. K. (1995). Interaction between focal adhesion kinase and Crk associated tyrosine kinase substrate p130Cas. *Proceedings of the National Academy of Sciences USA* 92: 10678-10682

57) Price, L., Leng, J., Schwartz, M. A., Bokoch, G. M. (1998). Activation of Rac and Cdc42 by Integrins mediates Cell Spreading. *Molecular Biology of the Cell* 9: 1863-1871

58) Raghunand, N., He, X., Van Sluis, R., Mahoney, B., Baggett, B., Taylor, C. W., Paine-Murrieta, G., Roe, D., Bhujwalla, Z. M., Gillies, R. J. (1999). Enhancement of Chemotherapy by Manipulation of Tumour pH. *British Journal of Cancer* 80: 1005–1011

59) Randazzo, P. A., Andrade, J., Miura, K., Brown, M. T., Long, Y. Q., Stauffer, S., Roller, P. and Cooper, J. A. (2000). The Arf GTPaseactivating protein ASAP1 regulates the actin cytoskeleton. *Proceedings of the National Academy of Sciences USA* 97: 4011-4016

60) Re, F., Zanetti, A., Sironi, M., Polentaruttie, N., Lanfrancone, L., Dejana, E., Colotta, F. (1994). Inhibition of Anchorage-Dependent Cell Spreading Triggers Apoptosis in Cultured Human Endothelial Cells. *The Journal of Cell Biology* 127: 2: 537-546

61) Rofstad, E. K., Mathiesen, B., Kindem, K. et al. (2006). Acidic Extracellular pH Promotes Experimental Metastasis of Human Melanoma Cells in Athymic Nude Mice. *Cancer Research* 66: 6699-6707

62) Rorth, P. (2009). Collective Cell Migration. *Annual Review of Cell and Developmental Biology* 25: 407-429

63) Rozhin, J., Sameni, M., Ziegler, G., Sloane, B. F. (1994). Pericellular pH affects distribution and secretion of cathepsin B in malignant cells. *Cancer Research* 54, 6517–6525

64) Saito, K., Ozawa, Y., Hibino, K., Ohta, Y. (2012). FilGAP, a Rho/Rho-Associated Kinase-Regulated GTPase-Activating Protein for Rac, Controls Tumor Cell Migration. *Molecular Cell Biology* 23: 24: 4739-4750

65) Sander, E. E., Klooster, J. P. T., Van Delft, S., Van Der Kammen, R. A., Collard, J. (1999). Rac Downregulates Rho Activity: Reciprical Balance between Both GTPases Determines Cellular Morphology and Migratory Behavior. *Journal of Cell Biology* 147: 5: 1009-1021

66) Schioth, H. B., Fredriksson, R. (2005). The GRAFS Classification System of G-protein Coupled Receptors in Comparative Perspective. *General and Comparative Endocrinology* 142: 94–101

67) Seuwen, K., Ludwig, M. G., and Wolf, R. M. (2006). Receptors for Protons or Lipid Messengers or Both? *Journal of Receptor and Signal Transduction Research* 26: 5-6: 599-610

68) Shibue, T., Brooks, M. W., Inan, M. F., Reinhardt, F., Weinberg, R. A. (2012). The Outgrowth of Micrometastases is Enabled by the Formation of Filopodium-like Protrusions. *Cancer Discovery* 2: 653-655

69) Sieg, D. J., Hauck, C. R., Schlaepfer, D. D. (1999). Required Role of Focal Adhesion Kinase (FAK) for Integrin-Stimulated Cell Migration. *Journal of Cell Science* 112: 2677-2691

70) Singh, L. S., et al. (2007). Ovarian Cancer G Protein-Coupled Receptor 1, a New Metastasis Suppressor Gene in Prostate Cancer. Journal of the National Cancer Institute 99:1313-1327

71) Slack, J. K., Adams, R. B., Rovin, J. D., Bissonette, E. A., Stoker, C. E. and Parsons, J. T. (2001). Alterations in the focal adhesion kinase/Src signal transduction pathway correlate with increased migratory capacity of prostate carcinoma cells. *Oncogene* 20: 1152-1163

72) Storr, S., Carragher, N., Frame, M., Parr, T., and Martin, S. (2011). The Calpain System and Cancer. *Nature Reviews Cancer* 11: 364-374

73) Strell, C., Entschladen, F. (2008). Extravasation of Leukocytes in Comparison to Tumor Cells. *Cell Communication and Signaling* 6: 10

74) Sun, X., Yang, L. V., Tiegs, B. C., Arend, L. J., McGraw, D. W., Penn, R. B., Petrovic, S. (2010). Deletion of the pH Sensor GPR4 Decreases Renal Acid Excretion. *Journal of the American Society of Nephrology* 21: 10: 1745-1755

75) Supuran, C. T. (2010) Carbonic anhydrase inhibitors. *Bioorganic Medicinal Chemistry Letters* 20: 3467–3474

76) Taylor, J. M., Hildebrand, J. D., Mack, C. P., Cox, M. E. and Parsons, J. T. (1998). Characterization of graf, the GTPase-activating protein for rho associated with focal adhesion kinase. Phosphorylation and possible regulation by mitogen-activated protein kinase. *Journal of Biological Chemistry* 273: 8063-8070

77) Taylor, J. M., Macklem, M. M. and Parsons, J. T. (1999). Cytoskeletal changes induced by GRAF, the GTPase regulator associated with focal adhesion kinase, are mediated by Rho. *Journal of Cell Science* 112: 231-242

78) Thiery, J. P., Acloque, H., Huang, R. Y. J., Nieto, M. A. (2009). Epithelial-Mesenchymal Transitions in Development and Disease. *Cell* 139: 871-890

79) Tobo, M., Tomura, H., Mogi, C., et al. (2007) Previously Postulated "Ligand-Independent" Signaling of GPR4 is Mediated through Proton-Sensing Mechanisms. *Cellular Signaling* 19: 1745-1753

80) Totsukawa, G., Wu, Y., Sasaki, Y., Hartshorne, D. J., Yamakita, Y., Yamashiro, S., Matsumura, F. (2004). Distinct Roles of MLCK and ROCK in the Regulation of Membrane Protrusions and Focal Adhesion Dynamics during Cell Migration of Fibroblasts. *Journal of Cell Biology* 2: 164(3): 427-439

81) Totsukawa, G., Yamakita, Y., Yamashiro, S., Hartshorne, D. J., Sasaki, Y., Matsumura, F. (2000). Distinct Roles of Rock (Rho-Kinase) and Mlck in Spatial Regulation of Mlc Phosphorylation for Assembly of Stress Fibers and Focal Adhesions in 3t3 Fibroblasts. *Journal of Cell Biology* 150: 4: 797-806

82) Valastyan, S., Weinberg, R. (2011). Tumor Metastasis: Molecular Insights and Evolving Paradigms. *Cell* 147: 275-292

83) Vaupel, P., Kallinowski, F., Okunieff, P. (1989). Blood flow, oxygen and nutrient supply, and metabolic microenvironment of human tumors: A review. *Cancer Research* 49: 6449-6465

84) Vaupel, P. (1992) Physiological properties of malignant tumours. *NMR in Biomedicine* 5: 220-225

85) Vaupel, P. (2004). Tumor Microenvironmental Physiology and Its Implication for Radiation Oncology. *Seminars in Radiation Oncology* 14: 3: 198-206

86) Wakatsuki, T., Wysolmerski, R. B., Elson, E. L. (2003). Mechanics of Cell Spreading: Role of Myosin II. *Journal of Cell Science* 116: 1617-1625

87) Warburg, O. (1956a). On the origin of cancer cells. *Science* 123: 309–314

88) Warburg, O. (1956b). On respiratory impairment in cancer cells. *Science* 124: 269–270

89) Warburg, O. H. (1930). The Metabolism of Tumours: Investigations from the Kaiser Wilhelm Institute for Biology, Berlin-Dahlem (London, UK: Arnold Constable)

90) Webb, B. A., Chimenti, M., Jacobson, M. P., and Barber, D. L. (2011). Dysregulated pH: A Perfect Storm for Cancer Progression. *Nature Reviews Cancer* 11: 671-677

91) Webb, D. J., Donais, K., Whitmore, L. A., Thomas, S. M., Turner, C. E., Parsons, J. T., Horwitz, A. F. (2003). FAK-Src Signaling Through Paxillin, ERK and MlcK Regulates Adhesion Disassembly. *Nature Cell Biology* 6: 154-161

92) Westoff, M. A., Fulda, S. (2009). Adhesion-Mediated Apoptosis Resistance in Cancer. *Drug Resistance Updates* 12: 127-136

93) Wyckoff, J. B., Wang, Y., Lin, E. Y., Li, J. F., Goswami, S., Stanley, E.R., Segall, J.E., Pollard, J.W., and Condeelis, J. (2007). Direct visualization of macrophage-assisted tumor cell intravasation in mammary tumors. *Cancer Research* 67: 6: 2649-2656

94) Yang, L. V. Radu, C. G., Roy, M., Lee, S., McLaughlin, J., Teitell, M., A., Iruela-Arispe, M. L., Witte, O. N. (2007). Vascular Abnormalities in Mice Deficient for the G-Protein-Coupled Receptor GPR4 That Functions as a pH Sensor. *Molecular Cell Biology* 27: 4: 1334-1347

95) Yang, L. V., Radu, C. G., Wang, L., Riedinger, M., Witte, O. (2005). Gi-Independent Macrophage Chemotaxis to Lysophosphatidylcholine Via the Immunoregulatory GPCR G2A. *Blood* 105: 3: 1127-1134

96) Yu, G. –L., Bradley, J. D., Attardi, L. D., and Blackburn, E. H. (1990). *In vivo* alteration of telomere sequences and senescence caused by mutated *Tetrahymena* telomerase RNAs. *Nature* 344: 126-132

97) Zaidel-Bar, R., Milo, R., Kam, Z., Geiger, B. (2006). A Paxillin Tyrosine Phosphorylation Switch Regulates the Assembly and Form of Cell-Matrix Adhesions. *Journal of Cell Science* 120: 137-148

98) Zhang, Y., Feng, Y., Justus, C. R., Jiang, W., Li, Z., Lu, J., Brock, R. S., McPeek, M., K., Weidner, D. A., Yang, L. V., Hu, X-H. (2012). Comparative Study of 3D Morphology and Functions on Genetically Engineered Mouse Melanoma Cells. *Integrative Biology* 4: 1428-1436

99) Zhao, G. and Rodriguez, B. L. (2013). Molecular Targeting of Liposomal Nanoparticles to Tumor Microenvironment. *International Journal of Nanomedicine* 8: 61-71